Sensitivity of Climate Change to Diapycnal Diffusivity in the Ocean

by

Fabio Dalan

Submitted to the Department of Earth, Atmospheric and Planetary Sciences
in partial fulfillment of the requirements for the degree of

Master of Science in Climate Physics and Chemistry

at the

MASSACHUSETTS INSTITUTE OF TECHNOLOGY

September 2003

Author .....
Department of Earth, Atmospheric and Planetary Sciences
August 15, 2003

Certified by .....
Peter H. Stone
Professor
Thesis Supervisor

Accepted by .....
Maria T. Zuber
Department Head
Department of Earth, Atmospheric and Planetary Sciences

Sensitivity of Climate Change to Diapycnal Diffusivity in the Ocean

by

Fabio Dalan

Submitted to the Department of Earth, Atmospheric and Planetary Sciences
on August 15, 2003, in partial fulfillment of the
requirements for the degree of
Master of Science in Climate Physics and Chemistry

Abstract

The diapycnal diffusivity of the ocean is one of the least known parameters in current climate models. Measurements of this diffusivity are sparse and insufficient for compiling a global map. Inferences from inverse methods and energy budget calculations suggests as much as a factor of 5 difference in the global mean value of the diapycnal diffusivity. Yet, the climate is extremely sensitive to the diapycnal diffusivity, as shown by studies using single-hemispheric ocean General Circulation Models (GCMs) and 2-dimensional coupled models. In this thesis we study the sensitivity of both the current climate and the climate change to the diapycnal diffusivity - using, for the first time, a coupled model with a 3-dimensional global ocean component and idealized geometry.

Our results show that, at equilibrium, the strength of the thermohaline circulation in the North Atlantic scales with the 0.44 power of the diapycnal diffusivity, in contrast to the theoretical value of 2/3. On the other hand, the strength of the circulation in the South Pacific scales with the 0.63 power of the diapycnal diffusivity. The implication is that the amount of water upwelling from the deep ocean may be regulated by the diapycnal diffusion in the Indo-Pacific ocean.

The vertical heat balance in the ocean is controlled by: in the downward direction, (i) advection and (ii) diapycnal diffusion; in the upward direction, (iii) isopycnal diffusion and (iv) bolus velocity (GM) advection. The size of the latter three fluxes increases with diapycnal diffusivity. The thickness of the thermocline also increases with diapycnal diffusivity leading to greater isopycnal slopes at high latitudes, and hence enhanced isopycnal diffusion and GM advection. Larger diapycnal diffusion compensates for changes in isopycnal diffusion and GM advection. Little changes are found for the advective flux because of compensation between changes in downward and upward advective fluxes.

We present sensitivity results for the hysteresis curve of the thermohaline circulation. The stability of the climate system to slow freshwater perturbations is reduced as a consequence of a smaller diapycnal diffusivity. This result confirms the findings of 2-dimensional climate models. However, contrary to the results of these studies, a

common threshold for the shutdown of the thermohaline circulation is not found in our model.

In our global warming experiments, the thermohaline circulation slows down for about 100 years and recovers afterward, for any value of the diapycnal diffusivity. The rates of slowdown and of recovery, as well as the percentage recovery of the circulation at the end of 1000-year integration, is variable but a direct relation with the diapycnal diffusivity cannot be found. The steric height gradient is divided into a temperature component and a salinity component. It appears that, in the first 70 years of simulated global warming, temperature variations dominate the salinity ones in weakly diffusive models, whereas the opposite occurs in strongly diffusive models.

The analysis of the vertical heat balance reveals that, in global warming experiments, deep ocean heat uptake is due to reduced upward isopycnal diffusive flux and GM advective flux. Surface warming, induced by enhanced CO_2 in the atmosphere, leads to a reduction of the isopycnal slope which translates into a reduction of the above fluxes. The amount of reduction is directly related to the magnitude of the isopycnal diffusive flux and GM advective flux at equilibrium. As mentioned above, the latter fluxes depend on the thickness of the thermocline at equilibrium, hence on the diapycnal diffusion. Thus, the increase of deep-ocean heat content with diapycnal diffusivity is an indirect effect that the latter parameter has on the isopycnal diffusion and GM advection.

Lastly, we analyze results from three climate GCMs involved in the Coupled Model Intercomparison Project. These GCMs have similar climate sensitivity to the MIT Earth Model of Intermediate Complexity (MIT-EMIC) but different rate of deep-ocean heat uptake. We find that the rates of change of surface air temperature and of sea level rise are comparable to those derived from the MIT-EMIC with different values of the diapycnal diffusivity. At the year of doubling CO_2, we estimate that an increase of the diapycnal diffusivity from 0.1 cm^2/s to 1.0 cm^2/s leads to a decrease in surface air temperature of about 0.4 K and an increase in sea level rise of about 4 cm.

Thesis Supervisor: Peter H. Stone
Title: Professor

Acknowledgments

"Ad Antonia e Delfina,

con tutto il cuore. "

I would like to thank my advisor Peter Stone for giving me the chance to work in his research group. He showed me how the complicate matter of climate science can be treated at various level of complexity and taught me, with his example, to constructively learn from the work of other people. For this I thank him. I also would like to thank Paola Malanotte for believing in me and for introducing me to EAPS and MIT. I am indebted to Igor Kamenkovich that, from the other side of US, patiently walked me through the meanders of ocean modeling. I thank Jeff Scott for leaving the door open to my innumerous questions and for often transforming doubts into motivation. I also thank Andrei Sokolov, Chris Forest, Boyin Huang and Stephanie Dutkiewicz for helping improving my work and for creating a friendly environment.

My experience at MIT has been enriched by the waves of "il Maestro" Joe Pedlosky, the QGPV of Kerry Emanuel, the Science of Ron Prinn and the Policy of Jake Jacoby, the momentum of Rick Rosen, the mixing of "DJs" Raffaele Ferrari and Glenn Flierl, the passion in their work of John Edmond and John Marshall, the pleasant discussions with Mick Follows, the example of Ed Lorenz and the forecasting course of (the multi-award holder) Lodovica Illari. Moreover, thanks to the free smiles of Lodo I had one more reason to come to work every day.

I thank EAPS students for rendering the MIT experience less traumatic, in particular my course-mates Valerio, for being what he is, Shin, for showing me that Italians and Japaneses are not so different, Tom for showing the good side of America and Americans, and Irene, for sharing with me this three-year experience. I cannot forget to thank Nikki for the plants, Tieh Yong and the "feline down the hall" for the cultural exchange, Paolina for the Italian conversations, Jonathan for backing me up against Sami, Zan and Jake for the parties, Kerim for the ski trip and EGSAC for the peers. As an EAPS student, I had the pleasure to work in contact with the staff

of the department. The care of Mary Elliff and the kindness of Carol Sprague and Joe Hankins I am most thankful for.

I would like to remember people that, in different ways, has been part of my life while in Boston, hoping that I am not forgetting anyone. I partied in Tang with: Afsheen, Ana, Aurelie, Ben, Benoit, Bukola, Cedric, Gustavo, Hazhir, Juan, Natalie, Noelle, Ping, Sergi, Theodoro. I hanged out in Somerville with: Alberta, Amy, Aron, Bukola, Diego, Gleb, Heather, Mike, Marko, Sherwin, Stephanie. We discussed on how steal money from the GSC with the Italian "mafia" Association: Antonio, Antonino, Antonello, Anna, *Bukola*, Carolina, Diego, Jacopo. I fought and drank with my friends in the MIT rugby team: Bill, *Bukola*, Dionisio, Michael, John, JP, Samuel, Steve, Willie (the coach), Wiggie and many other fine gentlemen.

My parents, my sister and my relatives, while patiently waiting for my return home, supported me anytime and in any ways they could. Thank you. Although far from my affections I have been blessed in finding the two most wonderful people. They have been my family and my friends. They shared with me happy and sad moments. I own them this thesis, three years of my life and an everlasting friendship. Thank you Samantha and JK[1].

[1]God Bless Venezuela, India and Italy.

Contents

List of Figures

List of Tables

Chapter 1

Introduction

In the present thesis we investigate the effect of diapycnal diffusivity on the climate system, both at equilibrium and in transient global warming experiments. This assessment is important in the framework of uncertainties of climate simulations, in view of the uncertainty of one of its least known parameters. Measurements of the diapycnal diffusivity in the Atlantic Ocean range from 5 cm^2/s above the mid-ocean ridge, to 0.1 cm^2/s over smooth topography (Polzin et al., 1997) and in the thermocline (Ledwell et al., 2000). However, these measurements are sparse both in space and time, thus a global value of the diapycnal diffusivity based on observations is not available. Inference from the density structure of the global ocean suggests that the global average diapycnal diffusivity is of the order of 1 cm^2/s (Munk (1966), Munk and Wunsch (1998)) while estimations of energy dissipation across the ocean give a global value closer to 0.2 cm^2/s (Huang, 1999). Still, ocean General Circulation Models (GCMs) use values for the diapycnal diffusivity ranging over an interval larger than the one given from measurements and calculations[1].

Several are the properties of the climate system potentially affected by the diapycnal diffusivity, both at equilibrium and in transient climate change simulations. We will focus our attention on the behavior of the Thermohaline Circulation (THC), the rate of ocean heat uptake and the stability of the climate under quasi-static freshwater

[1] According to CMIP2 (Coupled Model Intercomparison Project, see http://www-pcmdi.llnl.gov/cmip/cmiphome.html) documentation, for example, the Australian model from the Bureau of Meteorology Research Center assumes a constant diapycnal diffusivity of 20 cm^2/s.

perturbation.

1.1 Thermohaline Circulation

The THC is an important feature for the climate system responsible of transporting a significant amount of heat from the tropics towards the poles (Trenberth and Caron, 2001). Paleoclimatological studies often invoke the disruption of the THC as possible explanation of abrupt changes seen in the temperature proxy records.

The sensitivity of the present ocean circulation to the diapycnal diffusivity has been previously studied in ocean GCMs. The THC is more sensitive to the diapycnal diffusivity both at tropics and along the eastern and western boundaries (Scott and Marotzke, 2002), while in the vertical direction the sensitivity is high at the bottom of the thermocline (Cummins et al., 1990). These results have been confirmed also for a global Ocean GCM (OGCM) coupled to an energy balance model (Bugnion and Hill (2003a), their fig. 12 and Bugnion and Hill (2003b), their fig.8). Scott (2000) showed that the strength of the Thermohaline Circulation does not change considerably whether mixing is localized along the lateral boundaries or it is uniformly distributed over the ocean, as long as the area integrated diffusivity is the same in both cases. For the sake of simplicity, in the present study the diapycnal diffusivity is uniform across and within the ocean basins.

The sensitivity of the THC strength to the diapycnal diffusivity has been tested in single-hemisphere OGCMs with idealized topography (Bryan (1987), Zhang et al. (1999), Park and Bryan (2000)). A simple scaling argument comparing the strength of the THC and the diapycnal diffusivity holds in such models. According to it, the THC strengthens with increasing diapycnal diffusivity, following a power law relation of $2/3$. Analyzing the sensitivity of the current climate to changes in diapycnal diffusivity, we will revise the power-law relation of the THC in the context of a coupled model with a 3D global ocean component.

The THC is driven by the density contrast between North and South Atlantic (Hughes and Weaver, 1994). By changing the relative strength of the processes trans-

porting heat and salt in the ocean, positive feedbacks may strengthen, triggering strong non-linear behavior in the THC evolution. Changing the rate of CO_2 increase in the atmosphere, Stocker and Schmittner (1997) observed a slowdown and recovery of the THC or a complete collapse of the THC for slow and fast rates respectively. The same pattern was observed by Ganopolsky et al. (2001) varying both vertical diffusivity and hydrological sensitivity[2] in a 2.5D ocean model coupled with a 2D statistical dynamical model. For low vertical diffusivity and high hydrological sensitivity the THC shuts down in a simulation with 1% CO_2 rate of increase for 140 years and constant afterwards (stabilization at $4XCO_2$). For all the other combinations of the two parameters the strength of the THC decreases for about 150 years and then partially recovers. This study will extend Ganopolsky et al. (2001) results by using a 3D ocean model coupled with a 2D atmosphere and varying only the diapycnal diffusivity.

In transient global warming experiments, the THC strength does not change for certain models (Latif et al., 2000) or decreases for others (Dixon et al. (1999), Mikolajewicz and Voss (2000), Thorpe et al. (2001)). The evolution of the THC depends on both surface heat and moisture fluxes and the mechanisms by which these fluxes are transported in the sub-surface ocean (advection, diffusion and convection). In global warming experiments some models undergo larger changes in freshwater flux while in others the heat flux dominates the changes in the surface density field. Thus, the cause of the THC slowdown is attributed to changes in the freshwater flux in some models (Dixon et al., 1999) or to changes in the heat flux in others (Mikolajewicz and Voss (2000), Thorpe et al. (2001)). The MIT Earth Model of Intermediate Complexity (MIT-EMIC), model used in this thesis, falls in the latter category. Kamenkovich et al. (2003) proved that the density anomalies due to the heat flux entering the North Atlantic are about 7 time larger than the same anomalies due to the freshwater flux. Thorpe et al. (2001) carried out a detailed analysis of all the fluxes components that affects the steric height gradient decrease in the Atlantic Ocean in a global warming

[2]The hydrological sensitivity is defined as the ratio between the freshwater transport increase above 50N in the Atlantic Ocean and the North Hemispheric surface air temperature increase under global warming experiments.

simulation. The authors conclude that surface fluxes of heat and moisture decrease the steric height gradient while advection of heat and salt tend to increase it. However, the relative importance of these processes is highly dependent on the equilibrium state of the climate as well as on the formulation of the sub-grid scale parameterizations. One of the purposes of this study is to examine how the diapycnal diffusivity affects the strength of the processes regulating the density gradient between North and South Atlantic.

1.2 Ocean Heat Uptake

The purpose of the IPCC (Intergovernmental Panel on Climate Change) Working Group I is to make publicly available the current knowledge of the scientific community on the global warming issue. In the last IPCC report (Houghton et al., 2001), the results from model projections of the leading research groups are presented. Two of the most common physical quantities by which models are compared are: the rate of increase of Surface Air Temperature (SAT) and Sea Level Rise (SLR). All models simulate an increase in surface air temperature and sea level, as a consequence of an increase of CO_2 in the atmosphere, but the magnitude of the increase varies as much as a factor of three.

The rate of increase of SAT depends on the heat capacity of the Earth system. Because of the large heat capacity of water compared to air and land, the heat capacity of the combined atmosphere-land-ocean system depends on the portion of ocean that will be affected by global warming. The latter is regulated by the rate of ocean heat uptake. The sea level rises mainly because the volume of the water increases with temperature, therefore it also depends on the rate at which the ocean takes up heat (Sokolov and Stone, 1998). However the rate of ocean heat uptake is not well constrained by observations of the temperature record in the past 50 years (Forest et al., 2002) and greatly varies among models. Hence, sensitivity studies are needed in order to understand which processes and parameters control the rate of ocean heat uptake in numerical models.

Adjoint sensitivity studies show high sensitivity of the ocean heat content to isopycnal diffusive fluxes and bolus advective fluxes, both for the control climate (Huang et al., 2003a) and climate change (Huang et al., 2003c). However, varying both the isopycnal and thickness diffusivities does not change appreciably the rate of ocean heat uptake (Huang et al., 2003b). In this thesis, the sensitivity of the heat balance in the ocean to diapycnal diffusivity is presented. The sensitivity of such balance at equilibrium indicates whether the relative magnitude of the processes transporting heat vertically depends on the diapycnal diffusion. The sensitivity of the vertical balance under global warming experiments indicates if the rate of ocean heat uptake depends on diapycnal diffusion and shows which process is responsible for the increase of heat content in the ocean.

Gregory (2000) analyzed the heat balance of the vertical fluxes both at equilibrium and in a global warming experiment. The previous author combined together the advective fluxes (Eulerian and bolus velocity advection) and the diffusive fluxes (isopycnal and diapycnal) when analyzing the global ocean balance, while, investigating the balance for different latitude bands and basins, he limited the analysis to a single depth level (160 m). The heat balance at every depth level is presented by Huang et al. (2003a) and Huang et al. (2003b) for the equilibrium state and global warming scenario respectively. However the previous authors lump together the isopycnal diffusive flux and the bolus velocity advective flux. In the present study, the vertical heat flux of the ocean is divided into all its components and for every depth level.

Sokolov et al. (2003) mimicked the transient behavior of the global mean SAT and SLR of several 3D coupled Atmosphere-Ocean GCMs (AOGCMs) using a 2D atmospheric model coupled to a Q-flux mixed layer ocean of variable depth. Additionally, in the mixed layer heat is allowed to diffuse down into a non-dynamical deep ocean. The controlling parameters, used to match the transient response of the different climate models, were the strength of the cloud feedback and the rate of ocean heat uptake. The latter is controlled by an effective diffusivity parameter, that accounts for all processes responsible for transporting heat vertically in the ocean, namely:

advection, diffusion and convection. Using the Sokolov et al. (2003) model to fit the trend of the MIT-EMIC, we will be able to relate the diapycnal diffusivity and the effective vertical diffusivity and estimate the uncertainty of SAT and SLR solely due to the diapycnal diffusivity.

1.3 Quasi-static Freshwater Perturbation

Another interesting aspect of the climate system is its stability to freshwater perturbation. In hysteresis experiments the freshwater flux in the Atlantic Ocean increases (decreases) until the shutdown (recovery) of the THC is reached. The magnitude of freshwater flux increment is small enough so that the state of the model is always near the equilibrium. Hysteresis experiments are commonly performed to evaluate how far is the equilibrium climate of a model from the collapse of the THC due to enhanced freshwater flux in the North Atlantic.

According to the Clausius-Clapeyron law a warmer atmosphere is capable of holding more moisture and would draw more moisture out of the ocean. In the atmosphere, meridional transport of freshwater is mainly accomplished by mid-latitude baroclinic eddies whose strength can be parameterized as proportional to a latitude-dependent power of the meridional temperature gradient (Stone and Yao, 1990). In a global warming scenario the meridional temperature gradient is expected to decrease reducing the meridional heat transport. Between these two competing effects, the increase of moisture in the atmosphere and the decrease of the temperature gradient, the former effect seems to dominate (Manabe and Stouffer (1994)). Therefore hysteresis experiments, are investigating one of the possible phenomenon induced by a global warming scenario. However, these experiments are computationally expensive and sensitivity experiments of the hysteresis curve can be performed only with simplified models.

Ganopolsky et al. (2001) and Schmittner and Weaver (2001) performed hysteresis experiments given varying diapycnal mixing. Both studies show that the THC becomes more unstable for low values of the vertical diffusivity. Their results may

be biased by the use of models with a 2.5D ocean component. These models do not simulate the Coriolis force, hence the effect of rotation needs to be parameterize. Moreover, in 2.5D ocean models, important processes like convection and downward advection occurs at the same location while, in 3D ocean models with idealized topography, they occur at opposite sides of the Atlantic basin (Marotzke and Scott, 1999). Hence it is of interest to perform a sensitivity study of the hysteresis curve to diapycnal diffusivity, using a coupled model that includes a 3D ocean component.

1.4 Thesis Outline

The thesis is organized as follow: chapter 2 describes the numerical model used in this thesis. Chapter 3 contains the analysis of the equilibrium climate state; the sensitivity of the THC, vertical heat balance and hysteresis curve to the diapycnal diffusivity is presented. In chapter 4 the sensitivity of the transient climate state to the diapycnal diffusivity is outlined; here we analyze the behavior of the THC circulation and the rate of ocean heat uptake for simulations with different diapycnal diffusivity. Finally, chapter 5 contains a review of the major results in the thesis.

Chapter 2

MIT Earth Model of Intermediate Complexity

2.1 Atmospheric component

The 2-dimensional zonally averaged statistical-dynamical atmospheric model was developed by Sokolov and Stone (1998) on the basis of the GISS GCM (Hansen et al., 1983). The model solves the zonally averaged primitive equations in latitude-pressure coordinates. The grid of the model consists of 24 points in the meridional direction, corresponding to a resolution of 7.826°, and 9 layers in the vertical. Moreover, the model includes the parameterization of heat, moisture and momentum transports by large scale eddies (Stone and Yao, 1990) and has a complete moisture and momentum cycle.

Most of the physics and parameterizations of the atmospheric model derive from the GISS GCM. The 2D model, as well as the GISS GCM, allows four different types of surfaces in the same grid cell, namely: open ocean, sea-ice, land, and land-ice. The surface characteristics, as well as turbulent and radiative fluxes, are calculated separately for each kind of surface, while the atmosphere above is assumed to be well-mixed zonally. The atmospheric model uses a realistic land/ocean ratio for each latitude. More detailed description of the model can be found in Sokolov and Stone (1998) and Prinn et al. (1999).

The 2D atmospheric model coupled to a simple Q-flux mixed layer/diffusive ocean model has been shown to reproduce, under global warming experiments, the transient response in surface air warming and sea level rise, due to thermal expansion, as simulated by different coupled AOGCMs (Sokolov et al., 2003). The only two tunable parameters varied in this model are the cloud fraction, that controls the climate sensitivity, and an effective diffusion coefficient, that controls the heat penetration below the mixed layer. The dependence of zonal-mean surface fluxes of heat and momentum on surface warming simulated by the 2D model is qualitatively similar to that shown by more sophisticated atmospheric GCMs (Sokolov and Stone (1998); Prinn et al. (1999)). Moreover, vertical and latitudinal structure of the 2D model response is also consistent with the results of different GCMs. However, such a model cannot represent feedbacks associated with changes in the ocean circulation. To take into account possible interactions between atmosphere and ocean circulation, the diffusive ocean model is replaced, in this study, by a 3D ocean GCM with simplified geometry.

2.2 Ocean component

The ocean component of the coupled model is the MOM2 model (Pakanowski, 1996) with idealized geometry (fig. -1). It consists of two rectangular "pool" basins connected by the Drake Passage that extends from $64°S$ to $52°S$. The Indo-Pacific (hereinafter Pacific) pool extends from $48°S$ to $60°N$ and is 120° wide while the Atlantic pool extends from $48°S$ to $72°N$ and is 60° wide. Unrealistic land-ocean ratio is a consequence of the idealized geometry so small adjustments in the surface heat and moisture fluxes are needed to make the model energy and salt conservative.

The meridional resolution is 4° and the zonal resolution varies from 1° near the boundaries to 3.75° in the interior of the ocean. Better resolution of the boundary currents has been shown to improve the meridional heat transport in an ocean GCM (Kamenkovich et al., 2000). This advantage would be offset if we used a realistic geometry, because the realistic orientation of boundary currents would require increased

Parameter	Value	Units
Isopycnal Diffusivity	1000	$[m^2/s]$
Diapycnal Diffusivity	0.5	$[cm^2/s]$
Thickness Diffusivity	1000	$[m^2/s]$
Lateral Viscosity	50000	$[m^2/s]$
Vertical Viscosity	100	$[cm^2/s]$

Table 2.1: Sub-grid scale parameters of the ocean model in standard configuration.

resolution in both horizontal directions and therefore a significantly larger number of grid points. In the vertical, the model has 15 layers of increasing thickness from 53 m at the surface to 547 m at depth. The bottom of the ocean is flat and 4500 m deep everywhere except in the Drake Passage where there is a sill 2900 m deep.

No-slip conditions are applied to the lateral boundaries and free-slip at the bottom of the ocean, except in the Antarctic Circumpolar Current (ACC) where bottom drag is applied. Boundary conditions for tracers are insulating at lateral walls and bottom of the ocean. A mixed layer model adopted from the GISS GCM replaces the Ocean GCM southward of 64°S and northward of 72°N. The depth of the mixed layer is prescribed from observations as a function of latitude and time. In climate change simulations, heat penetrating into the ocean below the mixed layers is parameterized by diffusion of the deviation of the mixed layer temperature from its present-day climate values. Moreover, any changes in the runoff are evenly distributed throughout the ocean at any given time.

Gent McWilliams parameterization scheme is used to account for the small scale eddy induced transport (Gent and McWillams, 1990). Mixing caused by small scale process occurs along and across isopycnals. Hence, the mixing tensor is rotated to be aligned with the isopycnal slope (Redi, 1982). No background horizontal diffusivity is used. Table 2.2 summarizes the mixing parameters of the ocean model in its standard configuration.

The surface boundary conditions used to spin up the ocean model are taken from Jiang et al. (1999) who constructed the datasets using a variety of sources. Refer to their study for a complete description of the datasets. Mixed boundary conditions

are applied. The heat flux into the ocean is given by:

$$H_o^{spin}(x,y) = H^{obs}(y) + C\rho\frac{SST^{obs}(y) - SST(x,y)}{\lambda}d_1 \tag{2.1}$$

where H^{obs} is the observed heat flux, SST^{obs} is the observed Sea Surface Temperature (SST), zonally averaged and applied for each "pool" basin separately, λ is a restoring timescale of 60 days, d_1 is the depth of the ocean surface layer (53 m), C is the specific heat capacity, and ρ is the density of water. Note that the long-term average of the relaxation term would be zero if the model reproduced observed temperatures when forced by observed fluxes. This term therefore allows for correct representation of both heat fluxes and SST. Freshwater flux is specified from observations and no restoration of surface salinity is applied anywhere in the ocean.

Zonal means of all observed quantities are applied as boundary conditions (data from Indo-Pacific are used for the Pacific "pool"). Heat and freshwater fluxes are rebalanced to ensure zero net flux through the ocean surface. The SST, heat fluxes, and wind stress have a seasonal cycle, while the freshwater flux is annually averaged. For more details about the ocean model component refer to Kamenkovich et al. (2002).

2.3 Coupling, Spinup and Experiments Setup

Coupling takes place twice a day. The atmospheric model calculates 12-hour mean values of heat and freshwater fluxes over the open ocean (H_o,F_o), their derivatives with respect to the SST ($dH_o/dSST$, $dF_o/dSST$) and the wind stress. These quantities are then linearly interpolated to the oceanic grid. Heat and freshwater fluxes for the ocean model are:

$$Ht = H_o + (\frac{dH_o}{dSST})(SST - SST^*) \tag{2.2}$$

$$Fw = F_o + (\frac{dF_o}{dSST})(SST - SST^*), \tag{2.3}$$

where SST^* denotes the zonal average SST. The last term on the right-hand-side

relaxes the SST to its zonal average, allowing for the zonal variations of the fluxes as well as zonal transfer of heat and moisture among ocean basins. The last term in eq. (2.3) represents variations in evaporation only, i.e., there are no longitudinal variations in precipitation in our model. The wind stress is constant at each latitude.

The coupling procedure uses flux adjustments. From eqs. (2.2) and (2.3) the fluxes of heat (H_o) and freshwater (F_o) are:

$$H_o(x,y) = H_a(y) + [H_o^{spin}(x,y) - H_a^{obs}(y)] = H_o^{spin}(x,y) + [H_a(y) - H_a^{obs}(y)] \quad (2.4)$$

$$F_o(x,y) = F_a(y) + [F_o^{spin}(x,y) - F_a^{obs}(y)] = F_o^{spin}(x,y) + [F_a(y) - F_a^{obs}(y)], \quad (2.5)$$

The adjustments are given by the difference between the climatological fluxes, diagnosed after the spinup of the ocean-only model (H_o^{spin} from eq. (2.1)), and the climatological fluxes used to spinup the atmospheric model alone (H_a^{obs} and F_a^{obs}). Note that F_o^{spin} coincides with the observed freshwater flux since no restoration is applied to the surface salinity. Wind stress adjustment is calculated in the same way.

The ocean is integrated for 12 hours forced by the above fluxes and provides to the atmosphere the zonal mean SST. Asynchronous integration (Bryan, 1984) is used, with 12 hour time-step for the tracers equations and 1 hour time-step for the momentum equations. The coupled model takes about 4 hours to complete a hundred years integration in a 2.2 GHz Dell workstation with 2 GB memory.

After separate spinup of the atmospheric and oceanic components, forced by climatological SST and surface fluxes, the model has been coupled and spun up for 1000 years for each value of the diapycnal diffusivity: 0.1, 0.2, 0.5 and 1.0 cm^2/s. The model was considered to be at equilibrium when the global average heat flux entering the ocean fluctuates around the zero value. Peak-to-peak fluctuations of SAT are confined to two tenth of a degree and represent the natural variability of the climate as simulated by this model, comparable with what found in more sophisticated GCMs (Houghton et al. (2001), their fig. 12.1). The natural variability (estimated by the peak-to-peak variations) of the THC goes from few tenths of Sverdrups for

small diapycnal diffusivity, up to two Sverdrup for large diapycnal diffusivity, while in full 3D coupled GCMs the same quantity is of the order of 2-4 Sv (Houghton et al. (2001), their fig. 9.21).

The model has also been tested in direct coupling mode, where the ocean and atmosphere are coupled without the use of flux adjustments. Kamenkovich et al. (2002) tested the model in direct coupling mode using the standard value of the diffusivity and found that the model drifts towards an unrealistic equilibrium state. Direct coupling with 0.2 cm^2/s diffusivity has been tested to verify whether the model becomes more stable in this configuration. This is not the case since, after 200 years of integration, the equilibrium value for maximum overturning in the North Atlantic streamfunction drops down to less than 5 Sv.

In global warming experiments, the CO_2 in the atmosphere increases by 1% per year for 75 years and then it is kept constant for 925 years. Control runs are also performed starting at the end of the coupled spinup, with constant CO_2 concentration for 1000 years.

Chapter 3

Sensitivity of the equilibrium state

In this chapter we analyze the effect of changes in the diapycnal diffusivity on the equilibrium state of the climate model. In section 3.1 we look at the scaling behavior of the THC and the heat transport by the ocean, comparing our results with theoretical predictions and previous numerical studies. In section 3.2, the vertical heat balance in the ocean at equilibrium and its sensitivity to diapycnal diffusion is presented. Lastly, in section 3.3 we study the influence of diapycnal diffusivity on the hysteresis behavior of the THC.

3.1 Scaling Behavior

The sensitivity of the present ocean circulation to the diapycnal diffusivity has been previously studied in single-hemisphere single-basin OGCMs with idealized topography (Bryan (1987), Marotzke (1997), Zhang et al. (1999), Park and Bryan (2000)). A simple scaling argument relating the strength of the THC and the diapycnal diffusivity holds in such models. According to it (see Zhang et al. (1999) for a simple derivation), the thickness of the thermocline increases with the diapycnal diffusivity and, through the thermal wind relationship, the THC strengthens, following a power-law relation of 2/3.

Together with the THC strength, also the heat transport is easily derived by the same scaling argument. Assuming that the difference in temperature between the

surface and the bottom of the ocean (ΔT) is constant, the heat transport should be proportion to the strength of the THC and follow the same power-law. The study of Zhang et al. (1999) and Park and Bryan (2000) confirms this conclusion: the power-law dependence of the maximum heat transport on the vertical diffusivity is 2/3. However Marotzke (1997) finds a power of 1/2 arguing that this is due to the relation between ΔT and the strength of the overturning.

In this section we investigate the scaling behavior of our model for both the THC strength and heat transport. In doing so, we investigate whether the scaling argument holds also in coupled models with a 3D global ocean component.

3.1.1 Thermohaline Circulation

In the MIT-EMIC, the thermocline deepens and the THC strength increases (fig. -2, panels A to D), as predicted by the scaling argument first derived by Welander (1971), but with a power-law dependence between diapycnal diffusivity and THC strength of 0.44 (fig. -3). The power does not change considerably whether the global meridional streamfunction or the North Atlantic meridional streamfunction is considered since the overturning in the North Pacific is negligible (fig. -4, panels A to D). Moreover, after the spinup of the ocean alone, the overturning in the North Atlantic is only a few Sverdrup weaker than after the coupling with the atmosphere and the power-law is not much affected (fig. -3).

Contrary to single-hemisphere OGCMs, the scaling behavior of which agrees with the theory, the MIT-EMIC consists in a 3D global OGCM coupled with a 2D atmospheric model. In single hemisphere OGCMs water has to upwell in one basin while in the MIT-EMIC the upwelling occurs both in the Atlantic and the Pacific basins. In the latter basin, in particular, water sinks around 50S and upwells almost entirely in the tropical region (fig. -4, panels A to D). This overturning cell resembles more the one from a single basin model. In fact, the scaling of the South Pacific overturning with the diapycnal diffusivity shows a power-law dependence in better agreement with the scaling argument (fig. -5).

The scaling argument assumes an advective-diffusive balance in the oceans. Be-

cause of the greater area of the Pacific Ocean versus the Atlantic Ocean, it is reasonable to assume that, in the real world, most of the upwelling occurs in the Pacific Ocean. The work of Bugnion and Hill (2003b) (their fig. 8) supports this idea: the adjoint sensitivity of the THC strength to the diapycnal diffusion is greater in the tropical region of Atlantic, Pacific and Indian Ocean, implying greater vertical heat diffusion in the Indo-Pacific Ocean than in the Atlantic basin. Thus, it is suggested that the amount of vertical mixing in the Indo-Pacific ocean may be the factor controlling the strength of the overturning for a climate near an equilibrium state as in the present Holocene era.

Since the THC is an asymmetric feature of the ocean circulation subject to approximate symmetric forcing and considering our results, we speculate that inter-hemispheric and multi-basin extension of the ocean are the main causes for the difference between the power-law found here and the one holding in single-hemispheric single-basin OGCMs. For instance, the study of Knutti and Stocker (2000) (their fig. 5) shows a power-law dependence close to 1/2 with the use of a 2.5D ocean model coupled to an energy-balance model.

3.1.2 Heat Transport

In the Northern Hemisphere, the power-dependence between global ocean heat transport and diapycnal diffusivity is 0.24 (fig. -6). At the location of the maximum transport (from 18N for diffusivity 0.1 cm^2/s to 26N for diffusivity 1.0 cm^2/s), the strength of the meridional streamfunction for the global ocean depends on the 0.37 power of the diapycnal diffusivity (table 3.1). At the same location, the top-to-bottom temperature difference goes from 26°C, for diffusivity 0.1 cm^2/s, to 20°C, for diffusivity 1.0 cm^2/s, having a -0.12 power-dependence on the diapycnal diffusivity (table 3.1). The product of overturning strength and the top-to-bottom temperature explains the relation between the maximum heat transport and the diapycnal diffusivity (fig. -6). In our model, in fact, the main component of the poleward heat transport is given by the Thermohaline Circulation. Both in the spinup and coupling procedure the SST is restored to its zonal average, hence the heat transport by the

	Diapycnal Diffusivity	$[cm^2/s]$	0.1	0.2	0.5	1.0
A	Maximum heat transport	$[PW]$	0.72	0.84	1.08	1.25
B	Maximum streamfunction at A	$[Sv]$	11.4	12.8	19.8	26.0
C	Top-bottom temperature difference at A	$°C$	26.2	25.1	22.1	20.3

Table 3.1: Maximum heat transport (A), maximum streamfunction (B) and top-to-bottom temperature difference (C) for the global ocean. Both B and C are calculated at the location of maximum global ocean heat transport.

gyre circulation is greatly reduced. The absence of heat transport by the gyre circulation explains why the North Pacific contribution to the global heat transport in the Northern Hemisphere is negligible (fig. -7, panel C) and may also be the cause of the small power-dependence of the global poleward heat transport with the diapycnal diffusivity.

In the Southern Hemisphere, the dependence between the poleward heat transport and the diapycnal diffusion goes with the power of 0.45 for the global ocean and 0.35 for the Pacific component (not shown). Although the Pacific Ocean contributes the most to the global heat transport in the Southern Hemisphere, the Southern Atlantic contribution cannot be ignored (fig. -7, panels B, C). The latter is relatively insensitive to the diapycnal diffusivity explaining the decrease of power from the global ocean heat transport to the Pacific component in the Southern Hemisphere. The insensitivity of the Southern Atlantic heat transport to diapycnal diffusion may be relevant for the behavior of the THC. The strength of the THC is correlated with the steric height difference between the Northern and Southern Atlantic (Hughes and Weaver (1994), Thorpe et al. (2001)), which in turns is related to the integrated density over a water column. At each latitude, the heat transport, or better its divergence, affects the density of the water column thus the THC strength. This version of the MIT-EMIC has idealized geometry, in particular the African continent extends to 48S rather than a more realistic 30S. Moreover, no sea-ice model is included, hence processes like brine rejection, responsible for the formation of the Antarctic Bottom Water, are not modeled. Hence the insensitivity of the Southern Atlantic heat transport to the diapycnal diffusivity may be biased in our model. Further investigation

with a realist geometry coupled GCM is needed.

In general we find a smaller power-law dependence between oceanic heat transport and diapycnal diffusivity. Thus the uncertainties on the latter parameter reflect a smaller than thought uncertainty in the former quantity but the spread of values is still large (fig. -7, panel A). Our findings do not agree with the scaling argument either in the Northern Hemisphere or in the Southern Hemisphere. Two of the reasons for such a disagreement are underlined: the simplifications in the MIT-EMIC leads to an under-estimation of the gyre heat transport and the exclusion of important processes for the Southern Ocean circulation; the scaling argument may need to be revised to include more feedbacks in the ocean and possibly the atmosphere. In fact, as seen above, the top-to-bottom temperature difference affects the power-law for the Northern Hemisphere heat transport. The top-to-bottom temperature difference sensibly depends on the temperature of the water sinking in the North Atlantic which depends, among other things, on the ocean overturning circulation and both the atmospheric and oceanic meridional heat transports. The scaling argument, by its construction, cannot capture the relation between the top-to-bottom temperature difference, the strength of the overturning and the meridional heat transports.

3.2 Vertical Heat Balance

The analysis of the vertical heat balance in the ocean is a very useful tool for understanding ocean heat uptake and therefore ocean dynamics and thermodynamics. It, in fact, illustrates the importance of the various processes responsible for transferring heat in the vertical direction. Gregory (2000) analyzed the vertical heat balance of the ocean at a particular level (160 m) and considered the balance between total advection, total diffusion and convection. Huang et al. (2003a) illustrates the same balance for every depth (their fig.3) but does not separate the isopycnal diffusive component and the bolus advective component of the vertical heat flux.

In this section we perform a thorough analysis of the vertical heat balance for the current climate, dividing the heat fluxes into *all* its components, and we study the

sensitivity of the vertical heat balance to changes in diapycnal diffusivity. Following Gregory (2000) we divide the global ocean in three latitude bands: the Southern Ocean, southward of 30S, the tropics, between 30S and 30N and the Northern Ocean, northward of 30N. Investigating the vertical balance allows us to understand whether the changes in the circulation, caused by different diapycnal diffusivity in the model, induces a redistribution among the heat flux components. Moreover, the following analysis is indispensable for understanding what controls the rate of ocean heat uptake under global warming simulations. The analysis of the vertical heat balance under global warming experiments is presented in chapter 4, section 4.2.

3.2.1 Control Experiment

The vertical heat balance of the global ocean consists of downward diapycnal diffusion and eulerian advection (hereinafter advection) balancing upward fluxes by isopycnal diffusion and bolus velocity (hereinafter GM) advection (fig. -8, panel A). Convection plays a negligible role in all runs, the reason being explained at the end of this section.

Diapycnal diffusion, the major contributor to the downward heat flux for the global ocean (fig. -8, panel A), is concentrated in the tropical region although considerable diapycnal flux also occurs at high latitudes (same fig., panels B, C, D). However, while the tropical diapycnal flux is due to the presence of strong vertical temperature gradients, in high latitudes the diapycnal flux arises to partially compensate for the stronger and opposite isopycnal flux (same fig., panels B, D). Advection takes heat downward at high latitudes but mostly in the Northern Ocean (same fig., panels B, D) and upward in the tropics (same fig., panel C) so that the global contribution of the advective flux is the smallest among all the components[1] (same fig., panel A). Additionally, GM advection and isopycnal diffusion dominate at high latitudes, where the isopycnal slope is elevated (same fig., panels B, D).

In fig. -9, the heat flux components for the Northern Ocean and the tropics are separated for the Atlantic and Pacific basins. It is clear that the Northern Ocean fluxes are representative of the North Atlantic region, where most of the dynamics

[1] Excluding convection.

in this model takes place (same fig., panels A, B). Fluxes in the tropical Pacific are about twice as large as the tropical Atlantic ones, because the area extent of the former is twice the area of the latter (same fig., panels C,D). Fig. -8 and -9 do not include the surface heat flux, presented in fig. -10. Heat is entering in the tropical region at a rate of 13 Wm^{-2} (16 Wm^{-2} Atlantic and 11 Wm^{-2} Pacific) and leaving the ocean at high latitudes at a rate of -13 Wm^{-2} in the Southern Ocean and -23 Wm^{-2} in the Northern Ocean (-53 Wm^{-2} Atlantic and -4 Wm^{-2} Pacific).

Locally, downwelling occurs in the east side of the North Atlantic basin. The deep water formed in this region flows westward and southward for upwelling in the western side of the basin, as well as in the Southern Ocean and in the interior of the basins (fig. -11, panels A, C). Downward advection steepens the isopycnals generating elevated GM velocities. Hence, strong advective fluxes are contrasted by equally strong and opposite GM fluxes throughout the oceans (same fig., panels B, D). At high latitudes, diapycnal diffusion occurs in concert with isopycnal diffusion (fig. -12) partially compensating it as we have seen in fig. -8. The reason behind the compensation is the following: upward isopycnal fluxes cool the ocean and increase the vertical temperature gradient which is then relaxed by strong and localized downward diapycnal fluxes.

Gregory (2000) performed an analysis of the heat balance at 160 m depth for the HadCM2 climate model combining together the advective fluxes (Eulerian and GM) and diffusive fluxes (isopycnal and diapycnal). The author finds that, for the global ocean, downward heat advection is balanced by upward diffusion, opposite to the balance assumed in one-dimensional upwelling-diffusion models. In HadCM2, Southern Ocean fluxes dominate the global budget, thanks to a strong Deacon cell (47 Sv) that extends from 35S to 65S. Heat is taken down at 35S by advection and it is lost along the way by isopycnal diffusion. Water then upwells in much colder sites around 65S. In the MIT-EMIC the Deacon cell is significantly weaker (18 Sv) and its extension is limited between 48S and 64S. Although the vertical heat balance at different latitude bands in our model agrees with Gregory's (2000) picture (downward advection balances upward diffusion at high latitudes and the opposite at tropics), the

global budget for the MIT-EMIC is dominated by the tropical region, thus opposite to Gregory (2000) and in agreement with one-dimensional upwelling-diffusive models.

A convection-less model

Convection in this version of the MIT-EMIC is almost negligible. Such observation is against the conventional thinking that the Thermohaline Circulation cannot be sustained without convection in numerical models (Marotzke and Scott, 1999). The need for convection remains true if restricted to models with horizontal and vertical diffusion parameterization. Indeed, in such models, convection is the only means by which heat can be transported from the deep ocean to the surface. With the recent introduction of Redi and Gent-McWilliams parameterizations (Redi (1982), Gent and McWillams (1990)), both isopycnal mixing and bolus velocities can efficiently mix the upper ocean, inhibiting convection. This effect has been already noticed in 2D (Harvey (1995), their fig. 2) and 3D ocean models (Danabasoglu and Williams (1995), their fig. 22).

Reducing the isopycnal mixing and/or the bolus velocities would increase the ocean heat content and reduce the static stability. Convection should then take over. To prove that this is the case, we have performed two additional equilibrium experiments. From the control run with diapycnal diffusion 0.5 cm^2/s, we spun up the coupled model with reduced maximum isopycnal slope (from 0.01 of the standard model to 0.001) and with reduced isopycnal diffusion (from 1000 m^2/s to 100 m^2/s).

In the Reduced-Maximum-Slope (RMS) case, the maximum overturning in the Atlantic increases 2 Sv in comparison with the standard model (26 Sv), while the temperature structure is almost unchanged. Moreover, the GM streamfunction is reduced in the Southern Ocean but almost canceled in the North Atlantic, going from a maximum of 12 Sv to less that 4 Sv (fig. -13, panels A, B).

In the Small-Isopycnal-Diffusion (SID) case, the maximum overturning in the North Atlantic decreases by 2 Sv and the whole ocean warms up. The GM streamfunction is reduced by about 4 Sv, against the 8 Sv reduction of the RMS case (same fig., panels A, C). The introduction of the GM mixing scheme has been shown in the

past to improve the representation of the ocean circulation mainly in the Southern Ocean (Danabasoglu and Williams (1995), their fig. 4 and 5), thus a distribution of the bolus velocities as in the RMS case, with larger velocities in the Southern Ocean than in the Northern Ocean, agrees better with that reported in 3D GCMs with realistic geometry (Danabasoglu and Williams, 1995).

The heat balance of the Atlantic Ocean only is presented in fig. -14. In the RMS case both the isopycnal diffusive flux and GM advective flux are about half the control run fluxes (same fig., panels A, B). Compensating the reduction of these fluxes, a reduction of diapycnal diffusive fluxes and the appearance of upward convective fluxes is observed. Eulerian advection is virtually unchanged. In the SID case, the isopycnal diffusive fluxes decrease considerably, balancing the reduction of diapycnal diffusion (same fig., panels A, C). Convection plays a minor but not negligible role in the balance, while eulerian advection slightly increases at every depth level.

This result confirms that convective fluxes in the standard version of our model are being inhibited by GM advective fluxes and isopycnal diffusive fluxes. Greatly reducing the isopycnal diffusion only allows for convection to constitute a small term in the heat balance. However, reducing both isopycnal diffusion and GM advecton by 50% (accomplished by reducing the maximum slope of isopycnals) strongly enhances convective mixing. Therefore, we suggest that the GM fluxes are more efficient than the isopycnal fluxes in increasing the stability of the water column. Changing the isopycnal diffusivity and the maximum isopycnal slope involves also changes in the circulation pattern as well as in the surface heat flux distribution. We believe that these are second order effects in explaining the magnitude of the convective mixing, although further investigation is needed to support this conclusion.

3.2.2 Sensitivity to Diapycnal Diffusion

Four control experiments have been carried out, with the same model being spun up with different values of the diapycnal diffusivity, namely: 0.1, 0.2, 0.5 and 1.0 cm^2/s. Although the current estimates for the global average diapycnal diffusivity are 0.2 cm^2/s (Huang, 1999) and 1.0 cm^2/s (Munk and Wunsch, 1998), we compare

in detail the differences between the control runs with diapycnal diffusivity 0.1 cm^2/s and 0.5 cm^2/s, referring to the former case as the "small diffusivity model" and to the latter as the "standard diffusivity model". The conclusions drawn for the small diffusivity model can be applied to the simulations using diapycnal diffusivity 0.2 cm^2/s while the standard diffusivity case is similar, in its behavior, to the simulation with diapycnal diffusivity 1.0 cm^2/s. The reason behind the choice for diapycnal diffusivity 0.1-0.5 cm^2/s instead of 0.2-1.0 cm^2/s is that the former doublet gives a more representative range of where the strength of the THC in the real ocean may be found. The strength of the THC for the experiments with diapycnal diffusivity 0.1 and 0.5 cm^2/s is 12 and 26 Sv respectively while the latest estimates for the same quantity is 15 Sv (Ganachaud and Wunsch, 2003).

The vertical heat balance at equilibrium for the small diffusivity model is not much different from the standard diffusivity model. Isopycnal diffusion and GM advection dominate the removal of heat from the deep ocean at high latitudes while advection in the Northern Ocean is a major heat source for the deep ocean (compare fig. -15 with fig. -8). The major difference between the two simulations is in the tropical region. The diapycnal flux is significantly reduced in the small diffusivity model, as expected, and it is no longer the major heat source for the deep ocean, as it is for the standard diffusivity model (compare panels A,C of the above figures). Together with the reduction of the diapycnal flux, the upward advective flux is sensibly reduced. Hence, the downward advective flux for the global ocean slightly increases for the small diffusivity model against any intuition. In fact, the strength of the THC strongly decreases with decreasing diapycnal diffusivity (fig. -2). Nevertheless, compensation between decrease in downward warming at high latitudes and decrease in upward cooling in the tropics leads to small changes for the global advective flux. As for the standard diffusivity model, in the small diffusivity model the tropical region is dominated by the Pacific basin while the Northern Ocean is dominated by the Atlantic basin (not shown).

The magnitude of all fluxes is reduced with smaller diapycnal diffusivity (fig. -16) as expected from adjoint sensitivity studies (Huang et al. (2003a), their fig. 5 and 11).

Total advection always balances total diffusion since convection is always negligible in this version of the MIT-EMIC. Fluxes at the bottom of the first layer are 0.7 Wm^{-2} in the small diffusivity model (same fig., panel A) and one order of magnitude higher for the standard diffusivity model (same fig., panel C), rapidly decreasing with depth. Reduced diapycnal diffusion leads to smaller diapycnal fluxes and shallower thermocline at tropical latitudes (fig. -2). As a consequence, the isopycnal slopes at high latitudes are reduced and so are the isopycnal and GM fluxes. However, in the small diffusivity case, the tropics are no longer the dominant region at all depths, as it is for the standard diffusivity model, and in the upper 800 m of ocean and the advective-diffusive balance is reversed[2] (compare panels A, C of fig. -16).

3.3 Quasi-Static Freshwater Perturbation

The hysteresis cycle of the overturning circulation in the North Atlantic is an indication of the stability of the whole system to perturbation of freshwater flux. The cycle is constructed by increasing (reducing) the freshwater flux in the North Atlantic until the shutdown (recovery) of the THC is reached. Ganopolsky et al. (2001) and Schmittner and Weaver (2001) suggested that the stability of the climate system is reduced for a reduction in vertical diffusivity, i.e., the collapse of the circulation is achieved at a smaller freshwater perturbation, for small values of the vertical diffusion. Schmittner and Weaver (2001) noticed also that a common threshold of a minimum THC strength seems to exist, below which the circulation collapses. They conclude that the main reason for the early collapse in low vertical diffusion models is their smaller overturning in the equilibrium state. The equilibrium overturning strength for the current climate is proportional to the diapycnal diffusivity (Bryan, 1987) therefore also the salt transport into high latitudes. The latter helps sustain the Thermohaline Circulation, hence, the system is more unstable to freshwater perturbations for weaker equilibrium meridional circulation.

[2]The surface layer is subject to the surface boundary conditions. Here the heat flux from the atmosphere enters into the ocean as diffusive flux explaining the dominance of downward diffusion in the top layer of the model.

Both Ganopolsky et al. (2001) and Schmittner and Weaver (2001) used simplified coupled EMICs, in particular the ocean component is 2.5D. These models differ substantially from a 3D ocean model in several aspects, among which are the need to parameterize the effect of rotation, and the neglect of zonal variations in the North Atlantic. Convection and downward advection are particularly important for the behavior of the model under hysteresis experiments. These processes occur at the same latitude band in the North Atlantic, therefore, in 2.5D ocean models, convection and downward advection interact with each other, while in 3D ocean models with idealized topography they occur at opposite boundaries of the Atlantic Ocean, although at the same latitude (Marotzke and Scott, 1999).

Hence, it is of interest to perform hysteresis experiments for different values of diapycnal diffusivity, using a coupled model that includes a 3D ocean component. These hysteresis experiments have been carried out with the MIT-EMIC and the result is depicted in fig. -17. Note that in the hysteresis experiments the freshwater input is not balanced by any freshwater export in other regions of the ocean, therefore the global salinity of the ocean is not conserved. As in the aforementioned studies, the circulation is more unstable for a smaller value of the diapycnal diffusivity. In order to induce the THC to collapse, a freshwater input of 0.52 Sv is needed with diapycnal diffusivity of 0.5 cm^2/s while 0.37 Sv are needed with 0.2 cm^2/s diapycnal diffusivity. The THC collapses around 10 Sv in the standard diffusivity model (0.5 cm^2/s) and around 6 Sv in the low diffusivity model. A common threshold for the collapse does not seem to exist in this particular model, suggesting that the salt advection feedback only in part explains the early collapse of the THC. The Thermohaline Circulation resumes when the freshwater forcing in the North Atlantic is about 0.33 Sv, for diapycnal diffusivity 0.5 cm^2/s, and 0.23 Sv, for diapycnal diffusivity 0.2 cm^2/s.

For both values of the diapycnal diffusivity, the strength of the THC in the recovery process overshots the value obtained when increasing freshwater flux. This is indicative of a fast rate of decrease in the forcing. Two additional experiments has been carried out to verify the THC passes through quasi-steady states when the freshwater flux is increasing. For diapycnal diffusivity 0.2 cm^2/s, the freshwater flux has

been stabilized at 0.2 Sv and 0.3 Sv for 500 years. In both cases, the THC keeps on slowing down for about 100-150 years but it slightly recover and stabilizes within 300 years (not shown). Hence, the model can be considered to be in quasi-steady state for each value of the freshwater forcing. However, for sudden shifts in the regime of the circulation, the departure from equilibrium can be substantial. A slower rate of decrease in the freshwater flux would keep the model closer to equilibrium and avoid overshooting.

An accurate analysis of the stability under freshwater experiments goes beyond the purposes of this thesis. We limit ourselves to notice that the ocean circulation becomes more sensitive to freshwater perturbations as the diapycnal diffusivity decreases. To the extent that global warming experiments lead to an increase of freshwater in the North Atlantic (Manabe and Stouffer, 1994), the latter statement could be extended to global warming experiments as well. The distance of the equilibrium climate from the instability threshold is different among the different models (Rahmstorf et al, in prep.). For models close to the threshold, changing the amount of freshwater input in the North Atlantic, as a consequence of global warming, may lead to a collapse of the THC and the shift to an equilibrium with no water sinking in the North Atlantic (Ganopolsky et al. (2001), their fig. 11)..

Chapter 4

Sensitivity of the transient state

In this chapter we analyze the effect of changes in the diapycnal diffusivity on the transient state of a climate under global warming. In section 4.1 we look at the evolution of the THC and the processes responsible for its behavior. In section 4.2, the vertical heat balance in the ocean during global warming is broken down into all its component and the sensitivity to diapycnal diffusion is presented. Lastly, in section 4.3 the influence of diapycnal diffusivity on the rate of increase of surface air temperature and on sea level rise is investigated.

4.1 Behavior of the Thermohaline Circulation

The Thermohaline Circulation slows down as a consequence of enhanced CO_2 in the atmosphere, as simulated by several CMIP2 models (fig. -18). For each global warming simulation with different diapycnal diffusivity, the strength of circulation in the Atlantic Ocean decreases for 100 years, 25 years after the stabilization of the CO_2, and it recovers afterwards. Hence, the behavior of the system to changes in diapycnal diffusivity is self-similar. Ganopolsky et al. (2001) found strong non-linear behavior of the THC varying both vertical diffusivity and hydrological sensitivity[1]. For small vertical diffusivity and large hydrological sensitivity the THC shuts down

[1]The hydrological sensitivity allows one to regulate the amount of freshwater flux into the North Atlantic.

for a 1% CO_2 increase for 140 years, while for all other combinations of the two parameters the THC slows down and then partially recovers. Our model is extremely stable to freshwater perturbations, as inferred from the hysteresis curves of fig. -17. Moreover, we do not register major changes in freshwater flux in the North Atlantic as a consequence of global warming, which explains why in all our transient experiments the THC always recovers.

The rate and the amount of recovery vary for each experiment in an unpredictable way. For example, the simulation with diffusivity 0.5 cm^2/s presents the fastest recovery although it is with the diffusivity 0.2 cm^2/s that the circulation first fully recovers its strength (fig. -18). Moreover, the natural variability of the THC in the control run increases with the diapycnal diffusion, its value going from 0.2 Sv for the 0.1 cm^2/s diffusivity to 1 Sv for the 1.0 cm^2/s diffusivity. The behavior of the circulation depicted in fig -18 raises the question of the predictability of the THC in global warming experiments (Stocker and Schmittner (1997), Knutti and Stocker (2002)).

Regardless of the path followed in the recovery, the new equilibrium achieved after the CO_2 stabilization, presents a shallower overturning circulation (not shown), as noticed by Huang et al. (2003b). As a consequence of the THC slowdown, the bottom of the ocean fills up with cold water, which represents an obstacle for the water sinking in the North Atlantic when the circulation recovers.

The steric height is the integrated pressure from the surface to a reference depth, hence it is proportional to the the quantity:

$$P = \int_{z^*}^{0} \int_{z}^{0} \frac{\rho}{\rho_0} dz' dz, \tag{4.1}$$

where ρ is the in-situ density, ρ_0 is a reference density and z^* is a reference depth, in our case 3000m. The THC strength at equilibrium is correlated to the steric height difference between the North and South Atlantic (Hughes and Weaver (1994), Thorpe et al. (2001)). In the idealized geometry model of the MIT-EMIC, the steric height difference is not sensitive to the choice of the South Atlantic latitude, as long as the

latter is located northward of the Drake Passage, while the North Atlantic latitude needs to be north of 60N. The THC strength at equilibrium is best correlated to the steric height difference in the Atlantic Ocean when the latter is calculated between 30S and 66N-70N. Since, the THC circulation is stronger for increasing diapycnal diffusivity, the Gulf Stream extends to higher latitudes for the models with 0.5 and 1.0 cm^2/s diapycnal diffusivity. Hence, for a fair comparison among simulations with different diapycnal diffusivity, the steric height is calculated between 30S and 66N for diffusivities 0.1 and 0.2 cm^2/s and between 30S and 70N for diffusivities 0.5 and 1.0 cm^2/s.

Both the percentage reduction of the THC strength and steric height gradient decrease with increasing overturning (fig. -19). However the steric height gradient does not capture the fast recovery of the circulation for the model with diapycnal diffusivity 0.5 cm^2/s and also the percentage recovery at the end of the integration. This indicates that the longitudinal variations of the steric height may be relevant to explain the transient behavior of the THC.

Since the steric height depends on the density of the water column, we want to quantify the relative importance of the temperature and salinity profile in determining the steric height gradient. Using the temperature field from the transient run and the salinity field from the control run, we can calculate the temperature contribution to the steric height gradient. The salinity contribution is computed with the same technique. The result is depicted in fig. -20. For all simulations, the timeseries of the temperature and salinity contribution to the steric height gradient anomaly have a common trend, summarized as follows: at first, both temperature and salinity contributes to the decrease of the steric height gradient, while, after a certain timescale, temperature and salinity have opposite contribution to the steric height gradient (fig. -20). The timescale is regulated by the time at which the rate of change of the salinity contribution becomes positive, its value being roughly 140 years for the smallest diffusivities (0.1 and 0.2 cm^2/s) and for 70 years the largest diffusivities (0.5 and 1.0 cm^2/s). Therefore we can identify two types of systems: a slow responding system for small diffusivities and a fast responding system for large diffusivities.

Thorpe et al. (2001) carried out a detailed analysis of the changes in steric height gradient. The authors concluded that the surface fluxes of heat and freshwater tend to slowdown the THC, while the changes in the meridional heat and salt transport help the THC recovery. A preliminary analysis of our results suggests that the salinity fluxes in the deep ocean are greatly dominated by advection, both in the equilibrium and transient experiments. Thus, the response of the system seems to be related to the salinity advection feedback. For the temperature contribution the situation is more complicated. Changes in the GM advection and isopycnal diffusion tend to warm the North Atlantic as we will see in the next section. Moreover, the reduction of the THC implies a substantial reduction of the heat transport into high latitudes. This leads to a relative cooling of the North Atlantic and warming of the tropical Atlantic. Hence, changes in both GM advection and isopycnal diffusion decrease the steric height gradient while the decrease in meridional heat transport tends to increase it. Additionally, the contribution of the heat flux at the surface is about is about 7 times larger than the freshwater flux as shown by Kamenkovich et al. (2003), (their fig. 2a and 3).

An important characteristic of the response of the system is the relative role of temperature and salinity in determining the steric height gradient in the first 75 years of the transient runs. For slow responding systems, the temperature effect is always the dominant term (fig. -20, panels A, B). For fast responding systems, in the first decades of integration, the salinity anomalies has greater importance (same fig., panels C,D) than the temperature ones in determining the steric height gradient. At the time of doubling of CO_2 however, the changes in the temperature distribution in the ocean are driving the steric height gradient for all the global warming simulations.

The climate is a highly chaotic system, therefore the realizations portrayed in fig. -20 may strongly depend on the initial condition. To further investigate this aspect, we perform another global warming experiment with diapycnal diffusivity 0.5 cm^2/s starting from year 10 of the control run. The results can be seen in fig. -21. Starting from a different initial condition slightly changes the relative importance of temperature and salinity in the first 70 years of integration. In particular, in one

case the salt component of the steric height anomaly is larger than the temperature component for about 65 years of global warming (same fig., top panel); in the other case the dominance of the salt component extends over 70 years of integration (same fig., bottom panel). Note also that, in these particular realizations, the long term pattern is not affected by the initial condition.

A direct consequence of our observations is that fast responding models, i.e. with large equilibrium THC overturning, rather than slow responding models, may be more sensitive to changes in the salt content in the North Atlantic, as a consequence of enhanced CO_2 in the atmosphere. Hence, even for models showing the same surface heat and freshwater flux perturbations under global warming experiments, the sensitivities to the surface forcing may be different. The reason of such differences are most likely connected to the different strength of the advection feedback of the THC and the rate at which heat is taken up by the ocean. In the next section we will analyze the relation between the rate of ocean heat uptake and the diapycnal diffusivity.

4.2 Vertical Heat Imbalance

Because the ocean heat capacity exceeds the atmospheric and land heat capacity by several orders of magnitude, the rate at which ocean takes up heat determines the total heat capacity of the climate system as a whole. Such a rate influences the rate of increase of Surface Air Temperature (SAT) as well as the amount of heat absorbed by the ocean. The latter quantity is strongly related to the Sea Level Rise (SLR) due to thermal expansion. Both SAT and SLR are often compared among climate GCMs under global warming experiments and the spread in the results is considerable (Houghton et al., 2001). Sokolov et al. (2003) suggest that one of the reasons for disagreement among climate models may be their different rates of ocean heat uptake.

In this section we analyze the vertical heat imbalance for the climate change following Gregory (2000) and we study the sensitivity of such an imbalance to changes

in diapycnal diffusivity. In doing so we will address the following questions: what are the processes controlling the ocean heat uptake in global warming experiments? What is their relation with respect to the diapycnal diffusivity? Addressing these questions can help us understand whether differences in diapycnal diffusivity is one reason for the disagreement among the IPCC models in the matter of surface air temperature and sea level rise.

Moreover, the ocean heat uptake is an important factor in controlling the behavior of the THC under global warming experiments because it affects the temperature, and therefore the density, structure of the ocean. Hence, investigating the relationship between ocean heat uptake and diapycnal diffusivity may give some insight on the behavior of the THC under global warming experiments. In the previous section we have seen how the competition between temperature and salinity, in determining the steric height gradient, is affected by the diapycnal diffusivity. Here, we will investigate which process is responsible for the temperature change in the deep ocean as the CO_2 increases in the atmosphere.

4.2.1 Global Warming Experiment

In our global warming experiments the global ocean warms above 2500 meters and cools below this level (fig. -22, panel A). Cooling at depth occurs in the Northern Ocean (same fig., panel B) and it is due to the reduction of the THC with consequent reduction of downward advective heat transport in the North Atlantic. The reduction of upwelling in the tropics (same fig., panel C) compensates for the reduction of heating so that changes in the advective heat flux for the global ocean are negligible (same fig., panel A).

Heating in the upper 2500 meters is due to a decrease in both upward isopycnal diffusion and GM advection and it is concentrated at high latitudes (fig. -22, panels B, D), in agreement with the adjoint sensitivity study of Huang et al. (2003c) (their fig. 5). Surface heating in global warming experiments leads to less steep isopycnal slopes which explains the decrease in GM flux. Moreover, with increasing temperature, the density field becomes more dependent on the temperature field, because of

the non-linear dependence of the expansion coefficients on temperature and salinity. Hence, the angle between isopycnals and isotherms decreases, leading to a decrease of isopycnal temperature gradient and lastly of the isopycnal flux, as noticed also by Gregory (2000).

Surface warming leads to greater vertical temperature gradient and increased diapycnal diffusion in the tropical region (fig. -22, panel C). On the other hand, in dynamically active regions like the Northern and Southern Ocean the downward diapycnal flux decreases compensating the decrease of the upward isopycnal flux (same fig., panels B, D). As pointed out in section 3.2.1, the heat balance at the high latitudes has isopycnal diffusion and diapycnal diffusion acting in the same locations (fig. -12). Isopycnal diffusion removes heat from the deep ocean increasing the vertical temperature gradient. Diapycnal diffusion then relaxes this gradient by pumping heat downward. The opposite mechanism occurs in global warming experiments: reduction of isopycnal fluxes leads to warming at depth and relatively small vertical temperature gradient, which explains the decrease in downward diapycnal diffusion.

In fig. -23, the heat flux anomalies for the Northern Ocean and the tropics are separated for the Atlantic and Pacific basins. It is clear that the Northern Ocean anomalous fluxes are representative of the North Atlantic (same fig., panels A, B). The diapycnal flux anomaly in the tropical Pacific is about three times as large as in the tropical Atlantic because the area coverage of the Pacific is twice the Atlantic's, however the decreased upwelling in the tropics is greater in the tropical Atlantic than in the tropical Pacific (same fig., panels C, D).

The analysis of vertical heat fluxes in a global warming experiment is also presented by Gregory (2000). At 160 m depth the anomalous fluxes consist of: reduction of convection in the Northern Ocean, reduction of upwelling in the tropical region and reduction of upward isopycnal diffusion in the Southern Ocean. The total heat flux anomaly in the Southern Ocean and tropics are respectively 0.55 and 0.59 Wm^{-2}, more that three times the anomaly in the Northern Ocean (0.16 Wm^{-2}).

Qualitatively our results agree with Gregory (2000) in the tropics and in the Northern Ocean, noticing that in this model the role of convection is replaced by

GM advection and isopycnal diffusion, as shown in section 3.2.1. In the Southern Ocean we find that reduction of both isopycnal diffusion and GM advection are the major contributors to the increased heat flux. However, the Southern Ocean in the MIT-EMIC does not compare well with the one in a full 3D AOGCM for the reasons explained in section 3.1.2. Quantitatively, we notice that the vertical heat balance sensibly depends on depth (fig. -22). At high latitudes, the global heat flux anomaly decreases with depth from a value of 0.5 Wm^{-2} at the surface (same fig., panels B, D). At the tropics the anomaly is roughly constant at 0.2 Wm^{-2} between the surface and 2000 m for then decreasing with depth until the bottom of the ocean (same fig., panel C). Therefore, above 400 m both Northern and Southern Ocean contribute the most to the global heat flux anomaly, while below this level the tropics present the highest anomaly. At any given depth, our result do not agree quantitatively with Gregory (2000), the reasons to be sought in the differences among models.

Because the anomalous isopycnal and GM fluxes are the main contributors to the total anomalous heat flux (fig. -22, panel A), it is natural to think that, by changing isopycnal and/or thickness diffusivities, the amount of heat penetrating the ocean would change accordingly. This is not the case as Huang et al. (2003b) found. Employing the same version of the MIT-EMIC used in this study[2], the authors changed both isopycnal and thickness diffusivities by a factor of two. The anomalous heat flux from isopycnal diffusion and GM advection changes, although slightly, in the same direction of the parametric change (their fig. 11), and the total anomalous heat flux did not vary appreciably. Their anomalous vertical fluxes are in fact dominated by the reduction in convection and compensation in the changes of the other vertical heat components occurs. As we will see in the next section, the same does not happen when the diapycnal diffusion is changed, since total anomalous heat flux entering the ocean sensibly increases at all depths as the diapycnal diffusion increases.

[2]The MIT Ocean Model was used instead of MOM2.

4.2.2 Sensitivity to Diapycnal Diffusion

In global warming simulations the anomalous fluxes behave in the same way for all simulations given varying diapycnal diffusivity. (fig. -24). The major contributions to the heat uptake by the ocean are due to the reduction of isopycnal and GM fluxes at all depths. Moreover, the magnitude of the total anomaly is directly proportional to the diffusivity, implying a greater heat penetration for high diapycnal diffusivity (fig. -24). Indeed global ocean temperature increases more rapidly as the diapycnal diffusivity increases (fig. -29). However, the reason for the increase is not directly related to the increase of diffusive heat from the ocean surface, as common physical intuition might suggest. Maximum warming is localized at high latitudes of the Atlantic Basin and in the Southern Ocean (fig. -25), where isopycnal diffusion and GM advection dominate, both in magnitude in the control runs (fig. -8) and in tendency in global warming experiments (fig. -22). Note that the relative small warming at 50N in the Atlantic basin (fig. -25) is given by a southward shift of the Gulf Stream, as a consequence of the slowdown of the Thermohaline Circulation.

The connection between elevated diapycnal diffusivity and ocean heat uptake, given by isopycnal diffusion and GM advection, is found in the temperature structure of the ocean in the control run. The thickness of the thermocline is proportional to the diapycnal diffusivity, due to the larger heat diffusion from the surface of the ocean (fig. -2). Hence, at high latitudes the isopycnal slope increases as the thermocline deepens, followed by an increase of isopycnal and GM fluxes[3]. In global warming simulations, the surface warming reduces the isopycnal slopes (fig. -26) leading to a decrease of upward GM and isopycnal fluxes. The magnitude of the decrease is proportional to their control values, hence to the thickness of the thermocline and lastly to the diapycnal diffusivity.

4.3 Global Temperature and CMIP2 models

Sokolov and Stone (1998) developed a simplified 2D climate model, consisting of a 2D

[3]At equilibrium all fluxes increase for increasing diapycnal diffusion as inferred from fig. -16.

MIT-EMIC	Diapycnal Diffusivity	$[cm^2/s]$	0.1	0.2	0.5	1.0
MIT-2D model	Effective Diffusivity	$[cm^2/s]$	5	7.5	37.5	125

Table 4.1: Effective diffusivity of the MIT-2D climate model fitting the MIT-EMIC simulations with different diapycnal diffusivity.

atmospheric model derived from the GISS AGCM and a Q-flux mixed layer ocean with a non-dynamical deep ocean below it. Two parameters are particularly relevant is this model: the cloud fraction feedback, that controls the climate sensitivity of the model, and the effective vertical diffusivity of heat, that controls the rate of heat uptake by the ocean below the mixed layer. The effective vertical diffusivity represents the effect of advection, diffusion and convection, and it has a fixed meridional profile based on tritium measurements (Sokolov and Stone, 1998). By tuning these two parameters, the MIT-2D climate model can reproduce the trend of Surface Air Temperature (SAT) and Sea Level Rise (SLR) due to thermal expansion of the 3D GCMs involved in the CMIP2 Project (Sokolov et al., 2003). The MIT-EMIC uses the same atmosphere of the MIT-2D climate model whereas the ocean model is a full 3D OGCM. The MIT-2D climate model has been used to fit the trends of the MIT-EMIC. The values of effective diffusivity for the different experiments are reported in table 4.1.

Fig. -27 shows the position of the CMIP2 models and the MIT-EMIC in the two-dimensional parametric space of climate sensitivity (S) and the square root of the effective diffusivity [4] (k_v). The MIT-EMIC with different diapycnal diffusivities covers the whole range of effective diffusivities used to fit current 3D GCMs while its climate sensitivity is constant at 2.8 C. The climate sensitivity is not affected by the rate of heat uptake by the ocean, because the latter may change the rate at which temperature increases in the ocean and the atmosphere but not its equilibrium value. The climate sensitivity of the GISS-GR, HadCM2, HadCM3 and MRI1 models is particularly close to the climate sensitivity of the MIT-EMIC therefore a comparison can be made. The GISS-GR model, the least diffusive model among all, presents a rate of increase in SAT and ocean temperature very close to the MRI1 model

[4] Ocean heat uptake scales with the square root of the effective diffusivity (Sokolov et al., 2003).

(not shown), which is among the most diffusive models (fig. -27). Analyzing the streamfunction for the GISS-GR, it is found that the variability of the circulation in the control run exceeds the change associated with global warming. We believe that the GISS-GR model was not spun up to full equilibrium when the global warming simulation started. Therefore, this model has been left out from the following analysis to avoid misleading interpretations.

SAT trend is shown in fig. -28. Although SAT is very sensitive to the climate sensitivity (Kamenkovich et al. (2002), their fig. 13a and table 2), it can be inferred that the two versions of the Hadley Center model (HadCM2 and HadCM3) are less diffusive than the MRI1 model. A better indication of the diffusivity of a model is the rate of increase of temperature averaged over the whole ocean (fig. -29). Again it is clear that the MRI1 model is more diffusive than the Hadley center models, although a direct relationship between the effective diffusivity of the CMIP2 model and the diapycnal diffusivity of the MIT-EMIC cannot be made. The MRI1 model has a rate of temperature increase close to our simulation with diapycnal diffusivity 0.2 cm^2/s while, in the parametric space of climate sensitivity and effective diffusivity, this model seems closer to the simulation with diapycnal diffusivity 0.5 cm^2/s (fig. -27). The reason for the disagreement most likely lies in the different temperature distribution between our ocean model with idealized topography, in which no sea-ice is present at any time, and the one of the 3D-GCM.

The MRI1 model (Tokioka and Noda, 2001) uses a constant vertical diffusivity of 0.5 cm^2/s while the Hadley center models use a background vertical diffusivity linearly increasing with depth, from 0.1 cm^2/s at the surface to 1.5 cm^2/s at the bottom of the ocean (Johns et al., 1997). Additionally, the mixing schemes of Large et al. (1994) and Pakanowsky and Philander (1981) are implemented in HadCM3 (Gordon et al., 2000). The ocean circulation is more sensitive to value of the diapycnal diffusivity in the tropical region and below the thermocline, roughly around 100 m according to Bugnion and Hill (2003a) (their fig. 12 and 13). At this depth, the vertical diffusivity is 0.12 cm^2/s for the Hadley center models and 0.5 cm^2/s for the MRI1 model, values very close to the one used in the global warming simulations with the MIT-EMIC.

	Diapycnal Diffusivity	$[cm^2/s]$	0.1	0.2	0.5	1.0
A	SAT anomaly at year 70	$[K]$	1.83	1.68	1.57	1.46
B	SLR anomaly at year 70	$[cm]$	9.2	10.3	12.1	13.1

Table 4.2: Surface Air Temperature anomaly (A) and Sea Level Rise (B) at the time of doubling CO_2 for global warming experiments with different diapycnal diffusivity.

Thus, this analysis validates the results of the MIT-2D model in the context of the tri-dimensional dynamics of the ocean GCMs.

We can now estimate the uncertainty on SAT and SLR solely due to the parametric uncertainty on the value of the diapycnal diffusivity. The values are reported in table 4.2. At the time of doubling of CO_2, increasing the diapycnal diffusivity one order of magnitude leads to a decrease of SAT anomaly of about 0.4 K and an increase in SLR of about 4 cm.

Chapter 5

Conclusions

In the present thesis we analyzed the sensitivity of the climate to diapycnal diffusivity, for both equilibrium and global warming scenarios. This study is unique because the sensitivity to diapycnal diffusion of the ocean has not been investigated before using a coupled model with a 3D ocean component. We focused particularly on the behavior of the THC and on vertical heat balance in the ocean. Additionally, a first sensitivity study on the hysteresis cycle of the THC to the diapycnal diffusion is conducted for the 3D ocean model.

For the present climate state, the strength of the THC in the North Atlantic scales with the 0.44 power of the diapycnal diffusivity whereas a simple theoretical model predicts a power of 2/3. The theoretical model assumes vertical-diffusive balance in the ocean. Since the Pacific Ocean is about twice as large as the Atlantic Ocean most of the upwelling likely occurs in the former. Indeed, in our model, the Southern Pacific overturning does scale with the 0.63 power of the diapycnal diffusivity. Hence, we suggest that a controlling factor of the THC strength, for a climate close to equilibrium, is the value of the diapycnal diffusivity in the Pacific basin.

At equilibrium, the vertical heat balance of the global ocean is sensitive to the diapycnal diffusivity. Weaker mixing in the ocean leads to smaller diapycnal diffusive fluxes in the tropics and a thinner thermocline. As a consequence, isopycnal slopes at high latitudes are more gentle, leading to smaller isopycnal diffusive and bolus advective fluxes. Although the THC strength depends on the value of the diapycnal

diffusivity, compensation between high latitude downwelling and tropical upwelling means that changes of the total vertical advective flux are small. The relative importance of the fluxes at high latitude, compared to the fluxes in the tropical region, depends on the diapycnal diffusivity - the main cause being the reduction of diapycnal diffusion in the tropics. For elevated diapycnal diffusivity, the tropics dominates the global balance and the advective-diffusive balance is valid at all depths. For reduced diapycnal diffusivity, high latitude processes are relatively more important than low latitude ones and, for the global ocean, the advective-diffusive balance is reversed in the upper 800m.

More forward, we performed a sensitivity test of the hysteresis curve to the diapycnal diffusivity. As suggested by previous studies with 2D coupled model (Ganopolsky et al. (2001), their fig. 2b, Schmittner and Weaver (2001), their fig. 1), the THC becomes more unstable to freshwater perturbations for lower values of the diapycnal diffusivity. However, contrary to those studies, the threshold for the shutdown of the THC depends on the diapycnal diffusivity.

Increasing the carbon dioxide level in the atmosphere at a rate of 1% per year for 75 years leads to a slowdown of the THC circulation for about 100 years and recovery afterwards. The rate at which the circulation recovers and the percentage recovery at the end of the simulation vary with the diapycnal diffusion in an unpredictable fashion. For the largest (1.0 cm^2/s) and smallest (0.1 cm^2/s) values of the diapycnal diffusivity, recovery is slow and in-complete at the end of the 1000 years integration. For diapycnal diffusivity equal to 0.5 cm^2/s the recovery rate of the circulation is elevated, while for diapycnal diffusivity equal to 0.2 cm^2/s the circulation first recovers completely its control strength. For the first 60-70 years of integration, what differentiate the response of the climate system (as the diapycnal diffusion varies) is the relative contribution of temperature and salinity in determining the evolution of steric height gradient between North and South Atlantic. In climate systems with small diapycnal diffusivity, the temperature variations largely explain the changes in steric height gradient, while in highly diffusive ocean models the salinity variations dominates the temperature ones in terms of steric height. Thus, the sensitivity of

the model to surface heat and moisture flux depends on the diapycnal diffusivity. Both the strength of the THC and the thickness of the thermocline highly depends on the diapycnal diffusivity. As a consequences also the advective timescale and the magnitude of the GM advective fluxes and both isopycnal and diapycnal fluxes are related to the diapycnal diffusivity. Therefore the relation between sensitivity to surface forcing and diapycnal diffusivity is, mostly likely, and indirect consequence of the relation between the latter parameter and the state of the climate at equilibrium.

The rate of ocean heat uptake under global warming experiments increases with diapycnal diffusivity. The increase in ocean heat content is related to the decrease in bolus velocity (GM) advection and isopycnal diffusion, that are the major heat sinks. The role of convection is negligible in this version of the model since first GM advection and then isopycnal diffusion, efficiently mix the surface ocean. At high latitudes, the rise in sea surface temperature due to global warming leads to a decrease of isopycnal slope and in the temperature gradient along isopycnals. Consequently both GM advection and isopycnal diffusion are reduced inducing warming of the subsurface ocean. At equilibrium, the magnitude of the latter processes is greater for a thicker thermocline, thus for larger diapycnal diffusivity, as explained above. In global warming experiments the decrease in upward isopycnal diffusion and GM advection is proportional to their value at equilibrium, hence the rate of ocean heat uptake is larger for larger diapycnal diffusivity.

The uncertainty in the global value of the diapycnal diffusivity reflects on the uncertainty in ocean heat uptake under global warming scenarios, which in turn regulates the increase in Surface Air Temperature (SAT) and Sea Level Rise (SLR). Our calculations suggest that an increase of the diapycnal diffusivity by a factor 10 (from 0.1 cm^2/s to 1.0 cm^2/s) leads, at the time of doubling CO_2, to a decrease of SAT of 0.4 K and an increase of SLR due to thermal expansion of 4 cm.

Bibliography

Bryan, F. (1987). Paramenter Sensitivity of Primitive Equation Ocean General Circulation Models. *Journal of Physical Oceanography*, 17(7):970–985.

Bryan, K. (1984). Accelerating the convergence to equilibrium of ocean-climate models. *Journal of Physical Oceanography*, 14(4):666–673.

Bugnion, V. (2001). *Driving the Ocean's Overturning: an Adjoint Sensitivity Study.* PhD dissertation, Massachusetts Institute of Technology, Department of Earth, Atmospheric and Planetary Sciences.

Bugnion, V. and Hill, C. (2003a). The Equilibration of an Adjoint Model on Climatological Time scales. Part I: Sensitivity of Meridional Overturning Circulation to the Surface Boundary Conditions. *Journal of Climate*, Submitted.

Bugnion, V. and Hill, C. (2003b). The Equilibration of an Adjoint Model on Climatological Time scales. Part I: The Sensitivity of the Thermohaline Circulation to the Surface Forcing and Mixing in Coupled and Uncoupled Models. *Journal of Climate*, Submitted.

Cummins, P., Holloway, G., and Gargett, A. (1990). Sensitivity of the GFDL Ocean General Circulation Model to a Parameterization of Vertical Diffusion. *Journal of Physical Oceanography*, 20:817–830.

Danabasoglu, G. and Williams, J. C. M. (1995). Sensitivity of the Global Ocean Circulation to Parameterizations of Mesoscale Tracers Transports. *Journal of Climate*, 8(12):2967–2987.

Dixon, K., Delworth, T., Spelman, M., and Stouffer, R. (1999). The influence of transient surface fluxes on north atlantic overturning in a couple GCM climate change experiment. *Geophysical Research Letters*, 26(17):2749–2752.

Forest, C. E., Stone, P. H., Sokolov, A. P., Allen, M. R., and Webster, M. D. (2002). Quantifying Uncertainties in Climate System Properties with the Use of Recent Climate Observations. *Science*, 295:113–117.

Ganachaud, A. and Wunsch, C. (2003). Large-scale ocean heat and freshwater transports during the World Ocean Circulation Experiment. *Journal of Climate*, 16:696–705.

Ganopolsky, A., Petoukhov, V., Rahmstorf, S., Brovkin, V., Eliseev, A., and Kubatzki, C. (2001). CLIMBER-2: a climate model of intermediate complexity. part ii: model sensitivity. *Climate Dynamics*, 17:735–751.

Gent, P. and McWillams, J. (1990). Isopycnal Mixing in Ocean Circulation Models. *Journal of Physical Oceanography*, 20:150–155.

Gordon, C., Cooper, C., Senior, C. A., Banks, H., Gregory, J. M., Johns, T. C., Mitchell, J. F. B., and Woods, R. A. (2000). The simulation of sst, sea ice extents and ocean transport in a version of the hadley center coupled model without flux adjustments. *Climate Dynamics*, 16:147–168.

Gregory, J. M. (2000). Vertical heat transports in the ocean and their effect on time-depenent climate change. *Climate Dynamics*, 16:501–515.

Hansen, J., Russel, G., Rind, D., Stone, P., Lacis, A., Lebedeff, S., Ruedy, R., and Travis, L. (1983). Efficient three dimensional global models for climate studies: Model I and II. *Monthly Weather Review*, 111:609–662.

Harvey, D. L. D. (1995). Impact of Isopycnal Diffusion on Heat Fluxes and the Transient Response of a Two-Dimensional Ocean Model. *Journal of Physical Oceanography*, 25:2166–2176.

Houghton, J. T., Ding, Y., Griggs, D. J., Nouger, M., van der Linden, P. J., Dai, X., Maskell, K., and Johnson, C. A. (2001). *Climate Change 2001: The Scientific Basis.* Cambridge University press.

Huang, B., Stone, P. H., and Hill, C. (2003a). Sensitivity of deep ocean heat uptake and heat content to surface fluxes and subgrid-scale parameters in an OGCM with idealized geometry. *Journal of Geophysical Research*, 108:3015, doi:10.1029/2001JC001218.

Huang, B., Stone, P. H., Sokolov, A. P., and Kamenkovich, I. V. (2003b). Ocean Heat Uptake in Transient Climate Change: Mechanisms and Uncertainty due to Subgrid-Scale Eddy Mixing. *Journal of Climate*, Submitted.

Huang, B., Stone, P. H., Sokolov, A. P., and Kamenkovich, I. V. (2003c). The Deep-Ocean Heat Uptake in Transient Climate Change. *Journal of Climate*, 16(9):1352–1363.

Huang, R. X. (1999). Mixing and Energetics of the Oceanic Thermohaline Circulation. *Journal of Physical Oceanography*, 29:727–746.

Hughes, T. and Weaver, A. (1994). Multiple equilibria of an asymmetric two-basin ocean model. *Journal of Physical Oceanography*, 24:619–637.

Jiang, S., Stone, P. H., and Malanotte-Rizzoli, P. (1999). An assessment of the Geophisical Fluid Laboratory ocean model with coarse resolution: Annual-mean climatology. *Journal of Geophysical Research*, 104(C11):25623–25645.

Johns, T. C., Carnell, R. E., Crossley, J. F., Gregory, J. M., Mitchell, J. F. B., Senior, C. A., Tett, S. F. B., and Woods, R. A. (1997). The second Hadley Center coupled ocean-atmosphere GCM: model description, spinup and validation. *Climate Dynamics*, 13:103–134.

Kamenkovich, I. V., Marotzke, J., and Stone, P. H. (2000). Factors affecting heat transport in an ocean general circulation model. *Journal of Physical Oceanography*, 30:175–194.

Kamenkovich, I. V., Sokolov, A., and Stone, P. H. (2002). An efficient climate model with a 3D ocean and a statistical-dynamical atmosphere. *Climate Dynamics*, 19:585–598.

Kamenkovich, I. V., Sokolov, A., and Stone, P. H. (2003). Feedbacks affecting the response of the thermohaline circulation to increasing CO_2: a study with a model of intermediate complexity. *Climate Dynamics*, in press(DOI 10.1007/s00382-003-0325-5).

Knutti, R. and Stocker, T. F. (2000). The Effects of Subgrid-Scale Parameterizatons in a Zonally Averaged Ocean Model. *Journal of Physical Oceanography*, 30:2738–2752.

Knutti, R. and Stocker, T. F. (2002). Limited Predictability of the Future Thermohaline Circulation Close to an Instability Threshold. *Journal of Climate*, 15:179–186.

Large, W. G., McWilliams, J. C., and Doney, S. C. (1994). Oceanic Vertical Mixing: A Review and a Model with a Nonlocal Boundary Layer Parameterization. *Reviews of Geophysics*, 32:363–403.

Latif, M., Roeckner, E., Mikolajewicz, U., and Voss, R. (2000). Tropical stabilization of the thermohaline circulation in a greenhouse warming simulation. *Journal of Climate*, 13:1809–1813.

Ledwell, J. R., Montgomery, E. T., Polzin, K. L., Laurent, L. C. S., Schmitt, R. W., and Toole, J. M. (2000). Evidence of enhanced mixing over rough topography in the abyssal ocean. *Nature*, 403:179–182.

Manabe, S. and Stouffer, R. J. (1994). Multiple-Century Response of a Coupled Ocean-Atmosphere Model to an Increase of Atmospheric Carbon Dioxide. *Journal of Climate*, 7:5–23.

Marotzke, J. (1997). Boundary Mixing and the Dynamics of Three-Dimensional Thermohalina Circulation. *Journal of Physical Oceanography*, 27:1713–1728.

Marotzke, J. and Scott, J. R. (1999). Convective Mixing and the Thermohaline Circulation. *Journal of Physical Oceanography*, 29:2962–2970.

Mikolajewicz, A. and Voss, R. (2000). The role of the individual air-sea flux components in CO2-induced changes of the ocean's circulation and climate. *Climate Dynamics*, 16(8):627–642.

Munk, W. (1966). Abyssal recipes. *Deep Sea Reserch*, 13:707–730.

Munk, W. and Wunsch, C. (1998). Abyssal recipes II: Energetics of tidal and wind mixing. *Deep Sea Reserch*, 45:1977–2010.

Pakanowski, R. (1996). Mom2 version 2.0: Documentation user's guide and reference manual. Technical Report 3.2, Geophysical Fluid Dynamics Laboratory, Princeton, New Jersey.

Pakanowsky, R. C. and Philander, G. H. (1981). Parameterization of Vertical Mixing in Numerical Models of Tropical Oceans. *Journal of Physical Oceanography*, 11:1443–1451.

Park, Y.-G. and Bryan, K. (2000). Comparison of Thermally Driven Circulations from a Depth-Coordinate Model and an Isopycnal-Layer Model. Part I: Scaling-Law Sensitivity to Vertical Diffusivity. *Journal of Physical Oceanography*, 30(3):590–605.

Polzin, K. L., Toole, J. M., Ledwell, J. R., and Schmitt, R. W. (1997). Spatial Variability of Turbolent Mixing in the Abyssal Ocean. *Science*, 276:93–96.

Prinn, R., Jacoby, H., Sokolov, A., Wang, C., Xiao, X., Yang, Z., Eckaus, R., Stone, P. H., Ellerman, D., Melillo, J., Fitzmaurece, J., Kicklighter, D., Holian, G., and Liu, Y. (1999). Integrated global system model for climate policy assessment: feedbacks and sensitivity studies. *Climatic Change*, 41:469–546.

Redi, M. H. (1982). Oceanic isopycnal mixing by coordinate rotation. *Journal of Physical Oceanography*, 12:1154–1158.

Schmittner, A. and Weaver, A. (2001). Dependence of multiple climate states on ocean mixing parameters. *Geophysical Research Letters*, 28(6):1027–1030.

Scott, J. and Marotzke, J. (2002). The location of diapycnal mixing and the Meridional Overturning Circulation. *Journal of Physical Oceanography*, 32:3578–3595.

Scott, J. R. (2000). *The Role of Mixing and Geothermal Heating and Surface Buoyancy Forcing in Ocean Meridional Overturning Dynamics.* PhD dissertation, Massachusetts Institute of Technology, Department of Earth, Atmospheric and Planetary Sciences.

Sokolov, A. and Stone, P. H. (1998). A flexible climate model for use in integrated assessments. *Climate Dynamics*, 14:291–303.

Sokolov, A. P., Forest, C. E., and Stone, P. H. (2003). Comparing Oceanic Heat Uptake in AOGCM Trasient Climate Change Experiments. *Journal of Climate*, 16:1573–1582.

Stocker, T. F. and Schmittner, A. (1997). Influence of CO_2 emissions rates on the stability of the thermohaline circulation. *Nature*, 388:862–865.

Stone, P. H. and Yao, M.-S. (1990). Development of a Two-Dimensional Zonally Averaged Statistical Dynamical Model. Part III: The Parametrization of the Eddy Fluxes of Heat and Moisture. *Journal of Climate*, 3:726–740.

Thorpe, R. B., Gregory, J. M., Johns, T. C., Woods, R. A., and Mitchell, J. F. B. (2001). Mechanisms Determining the Atlantic Thermohaline Circulation Response to Greenhouse Gas Forcing in a Non-Flux-Adjusted Coupled Climate Model. *Journal of Climate*, 14:3102–3116.

Tokioka, T. and Noda, A. (2001). Global Warming Projection Studies at the Meteorological Research Institute/JMA. In Matsuno, T. and Kida, H., editors, *Present and Future of Modeling Global Environment Change: Toward Integrated Modeling*, pages 1–14. TERRAPUB. http://www.terrapub.co.jp/e-library/toyota/pdf/001.pdf.

Trenberth, K. E. and Caron, J. M. (2001). Estimates of Meridional Atmosphere and Ocean Heat Transport. *Journal of Climate*, 14:3433–3443.

Welander, P. (1971). The Thermocline Problem. *Philosophical Transactions of the Royal Society of London. Series A, Mathematical and Physical Sciences*, 270:415–421.

Zhang, J., Schmitt, R. W., and Huang, R. X. (1999). The Relative Influence of Diapycnal Mixing and Hydrological Forcing on the Stability of the Thermohaline Circulation. *Journal of Physical Oceanography*, 29(6):1096–1108.

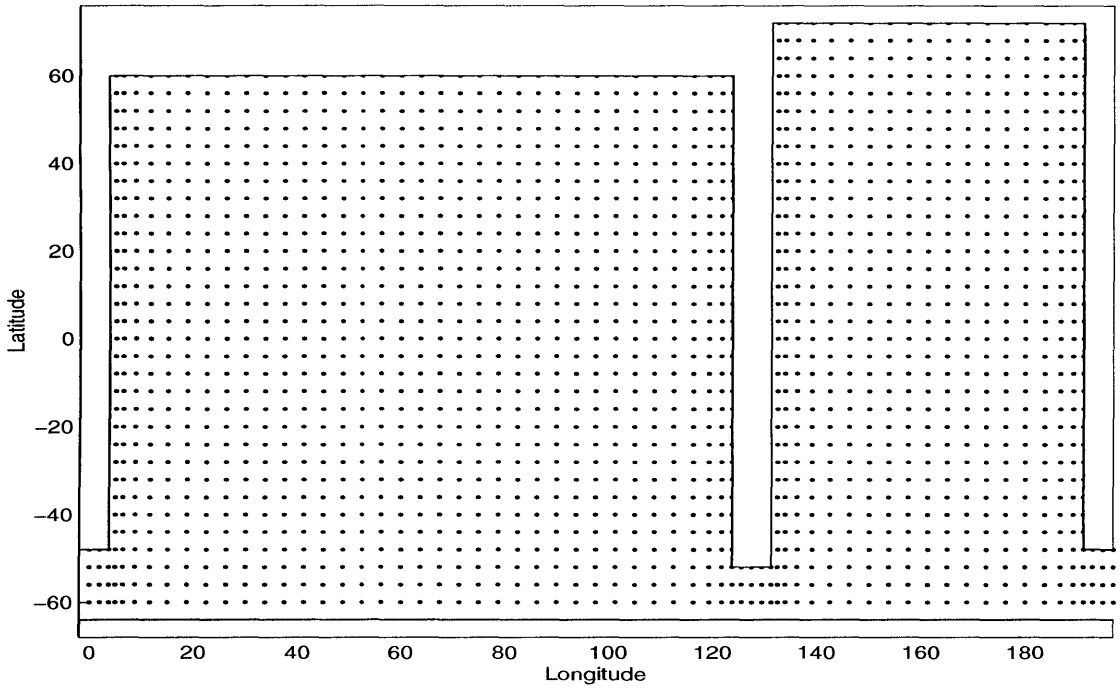

Figure -1: Geometry of the ocean model and velocity points in the Arakawa B-grid.

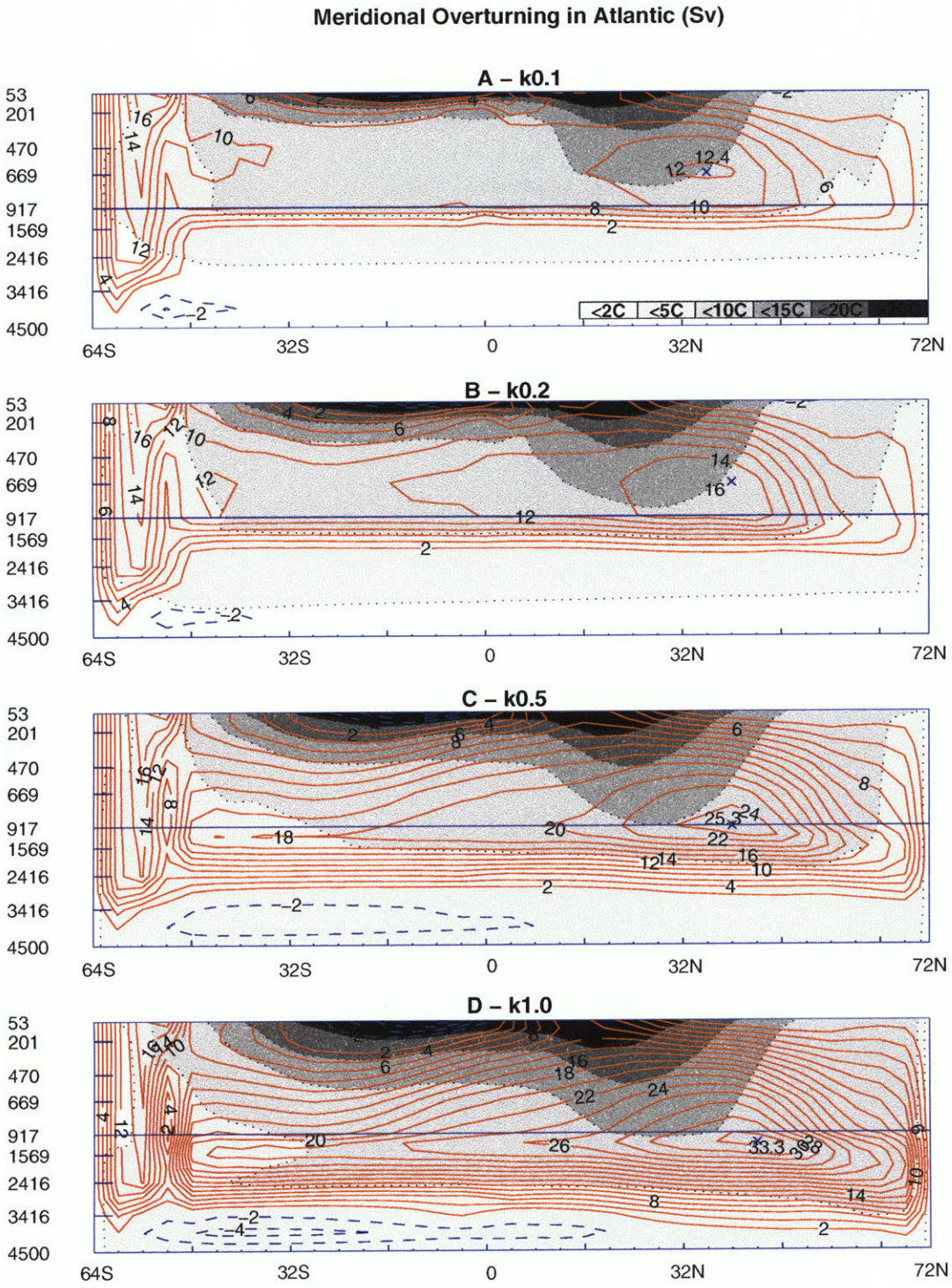

Figure -2: Meridional streamfunction of the Atlantic Ocean at equilibrium for diapycnal diffusivity 0.1 cm^2/s (panel A), 0.2 cm^2/s (panel B), 0.5 cm^2/s (panel C), 1.0 cm^2/s (panel D). South of the 48S the global ocean streamfunction is plotted. Solid line for clockwise overturning and dashed line for anticlockwise overturning. Shading indicates temperature according to the scale in panel A.

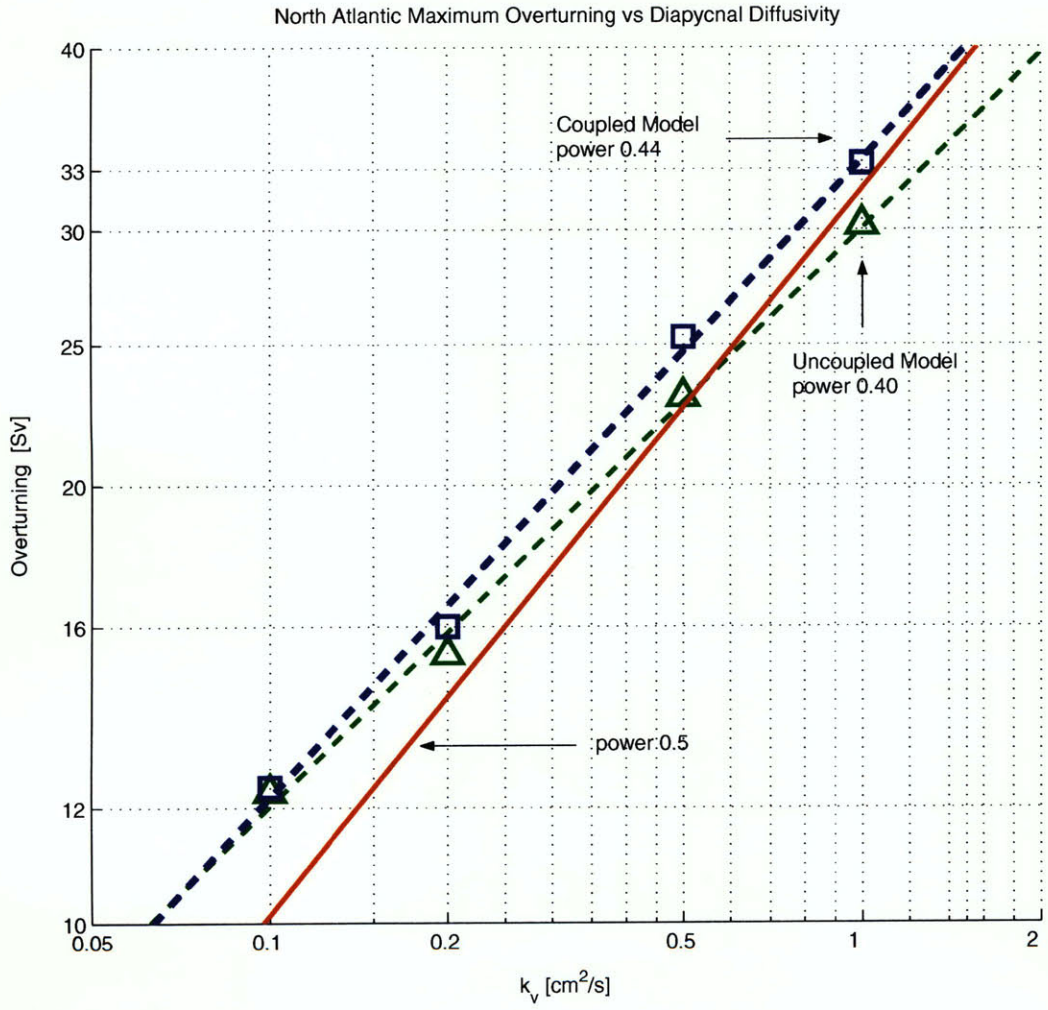

Figure -3: Maximum in the meridional streamfunction of the North Atlantic Ocean for coupled (squares) and uncoupled (triangles) model at equilibrium versus diapycnal diffusivity (k_v). Log-Log plot. Linear regression lines are dashed while the solid line shows the relation $(k_v)^{0.5}$ for comparison.

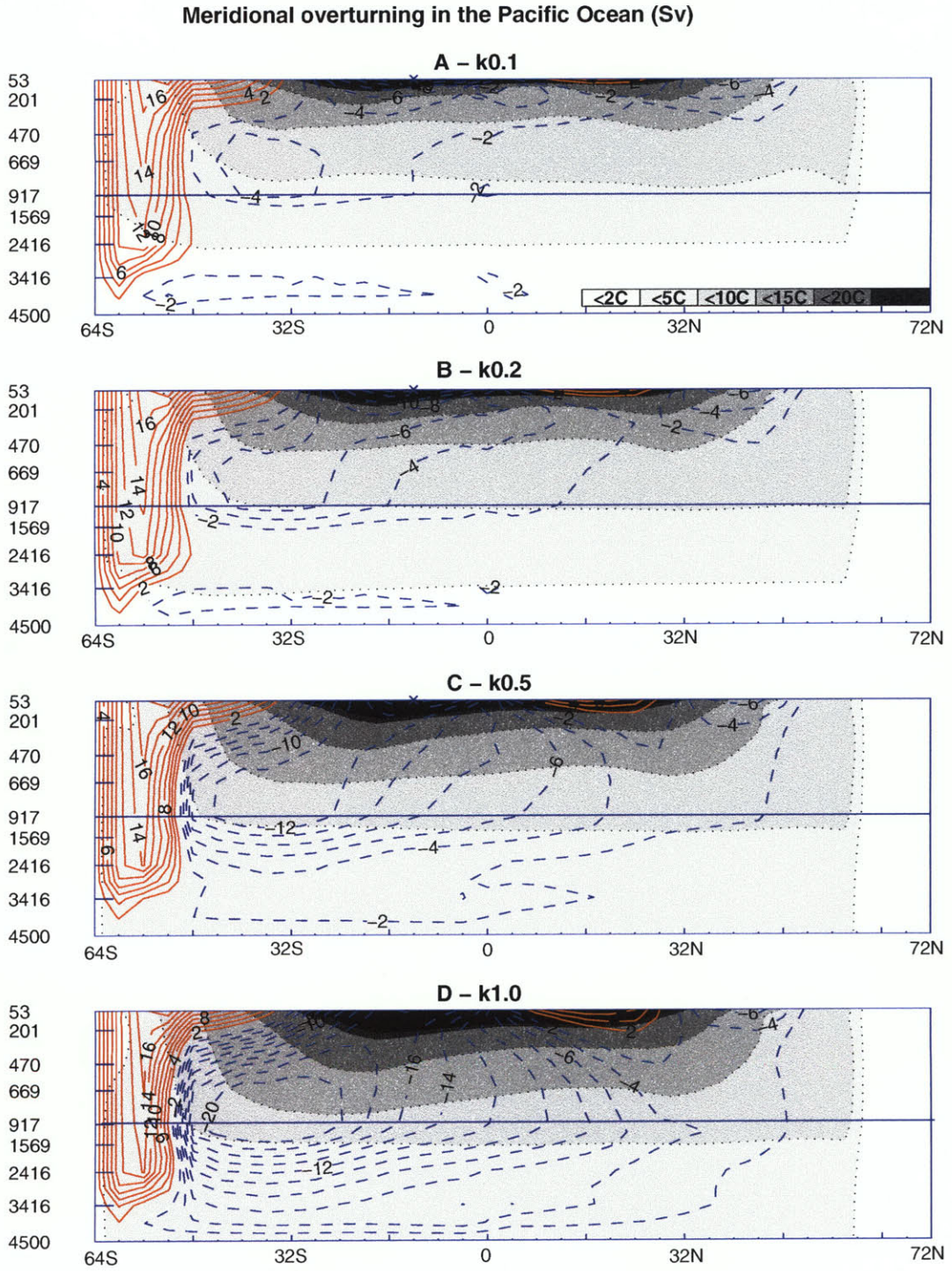

Figure -4: Meridional streamfunction of the Pacific Ocean at equilibrium for diapycnal diffusivity 0.1 cm^2/s (panel A), 0.2 cm^2/s (panel B), 0.5 cm^2/s (panel C), 1.0 cm^2/s (panel D). South of the 48S the global ocean streamfunction is plotted. Solid line for clockwise overturning and dashed line for anticlockwise overturning. Shading indicates temperature according to the scale in panel A.

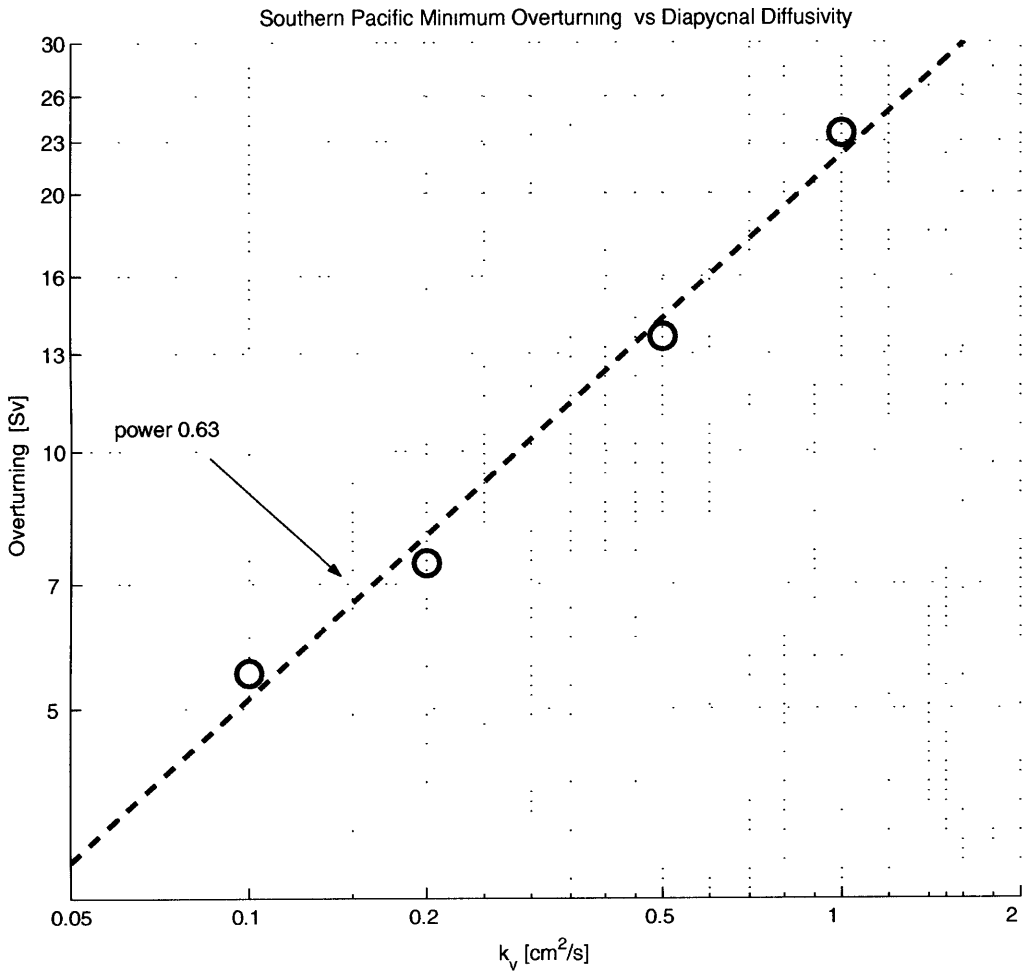

Figure -5: Minimum in the meridional streamfunction of the South Pacific Ocean (circles) at equilibrium versus diapycnal diffusivity (k_v). Log-Log plot. Linear regression line is dashed.

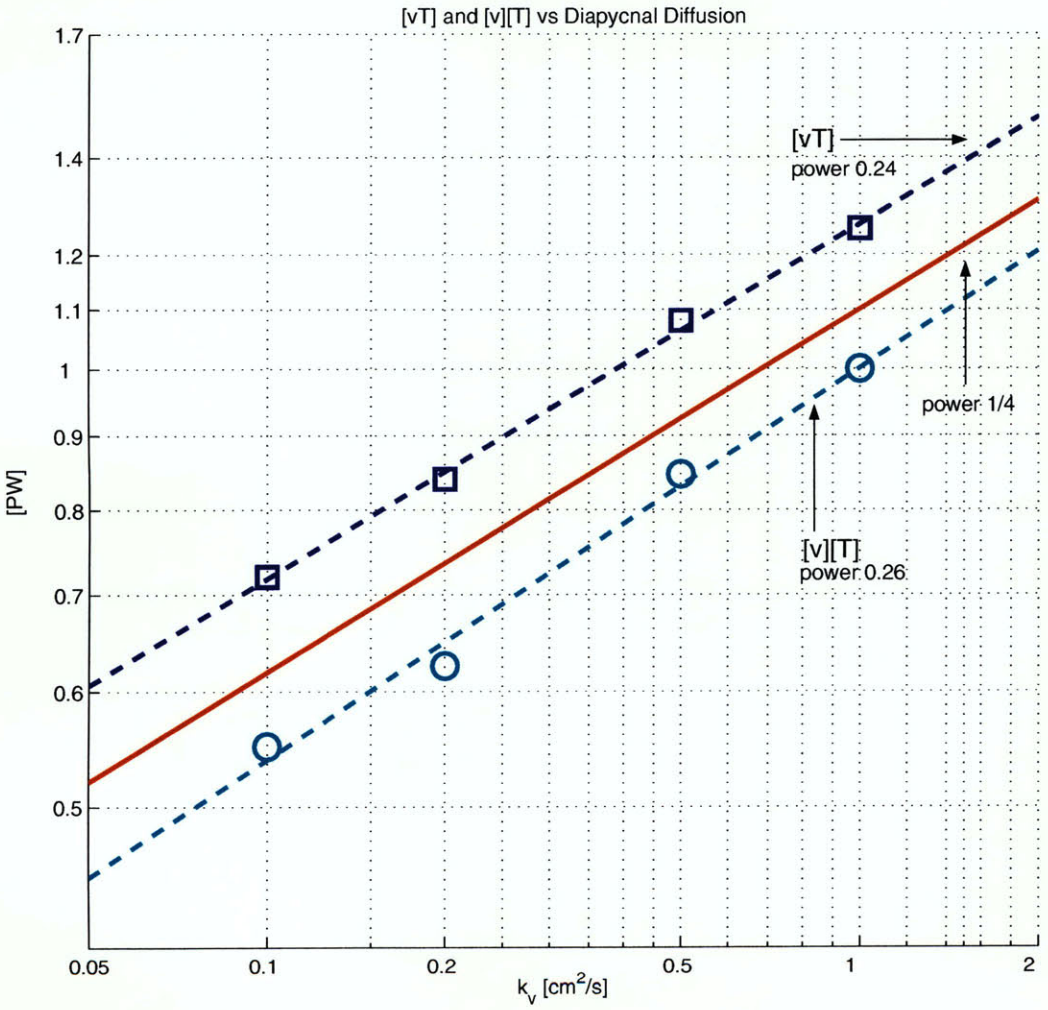

Figure -6: Maximum poleward heat transport ([vT], squares) and heat transport by the mean meridional circulation ([v][T], circles) for the global ocean at equilibrium versus diapycnal diffusivity (k_v). Log-Log plot. Both [v] and [T] are normalized by their value at diffusivity 1.0 cm^2/s. Linear regression lines are dashed while the solid line represent the relation $(k_v)^{0.25}$.

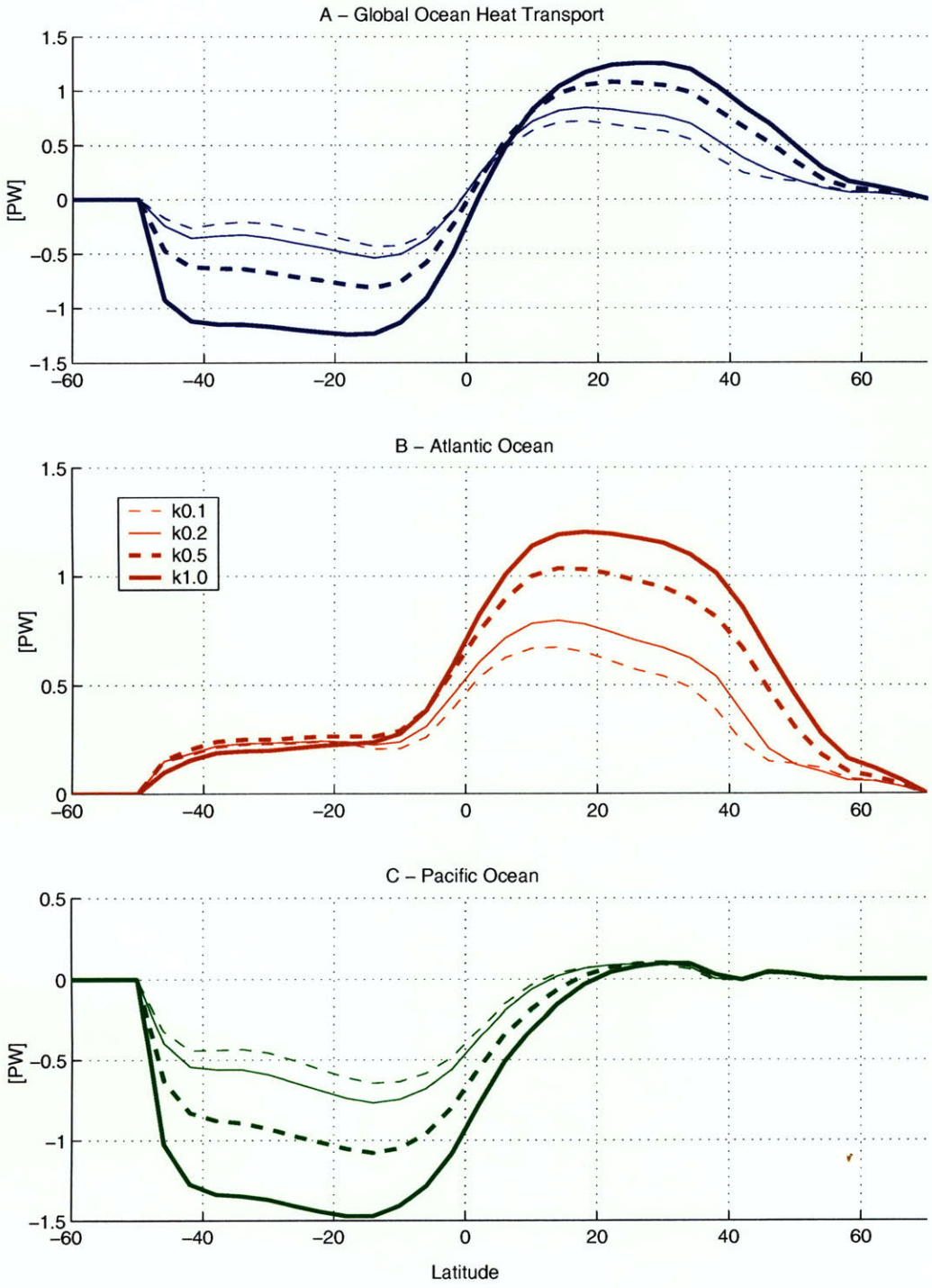

Figure -7: Poleward heat transport for the global ocean (top), Atlantic Ocean (middle) and Pacific Ocean (bottom) for diapycnal diffusivity 0.1 cm^2/s (thin dashed line), 0.2 cm^2/s (thin solid line), 0.5 cm^2/s (thick dashed line) and 1.0 cm^2/s (thick solid line).

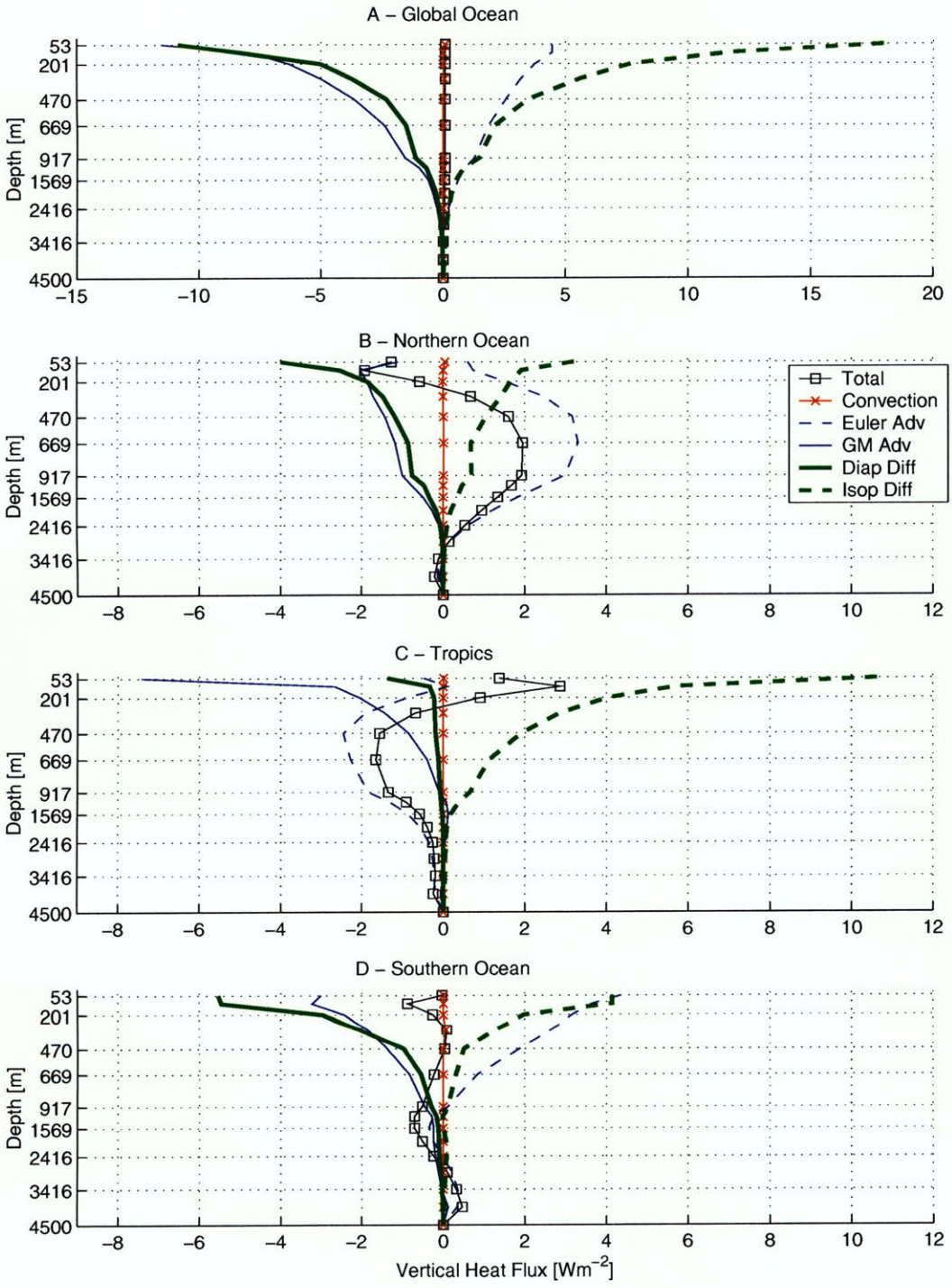

Figure -8: Control Run. Vertical heat flux components for global ocean (A), Northern Ocean (B), Tropics (C) and Southern Ocean (D) for diapycnal diffusivity 0.5 cm^2/s. Positive (negative) sign for downward (upward) fluxes. Note the change of scale in panel A.

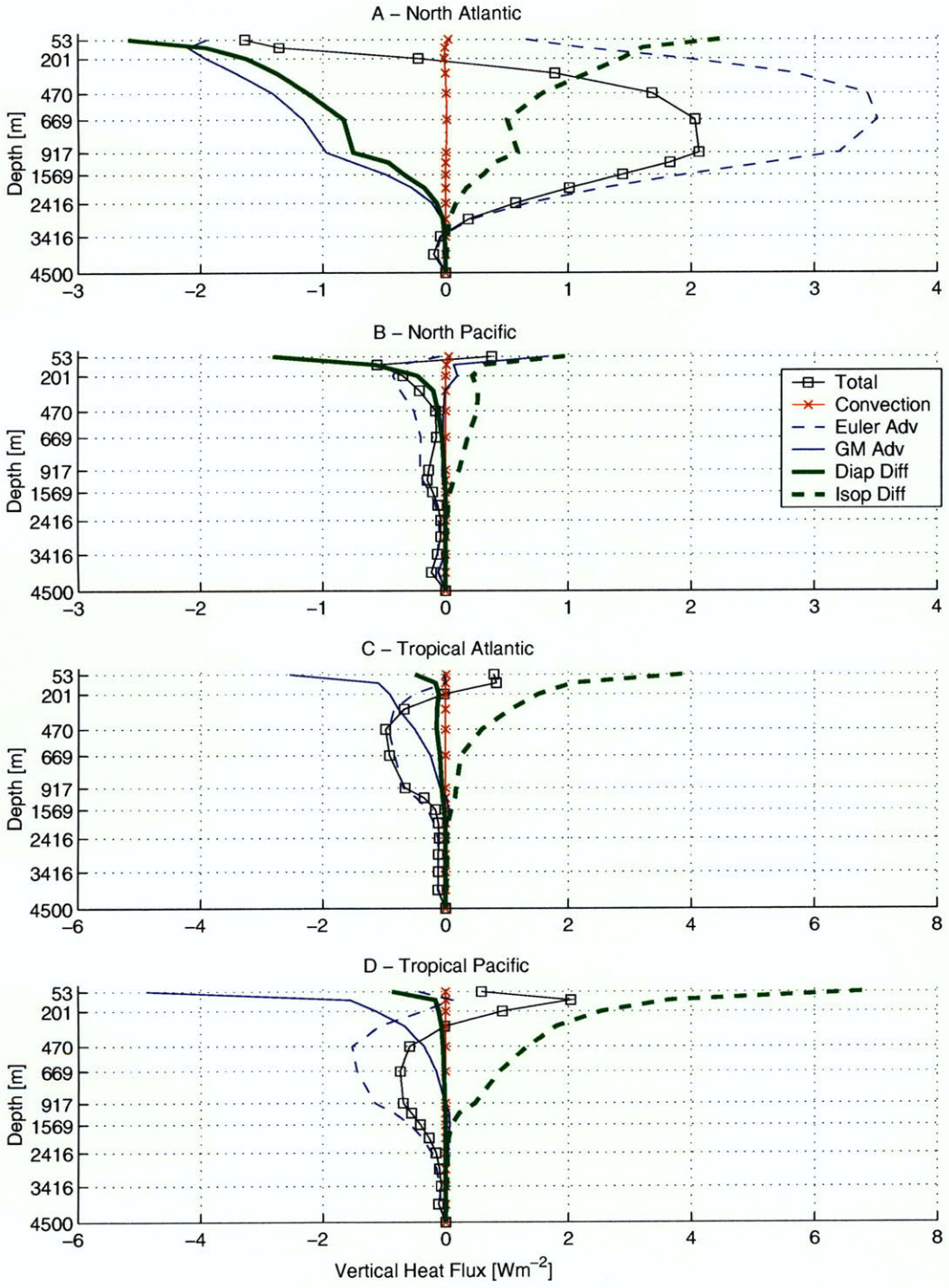

Figure -9: Control Run. Vertical heat flux components for the North Atlantic (A), North Pacific (B), tropical Atlantic (C) and tropical Pacific (D) for diapycnal diffusivity 0.5 cm^2/s. Positive (negative) sign for downward (upward) fluxes. Note the change of horizontal scale among panels.

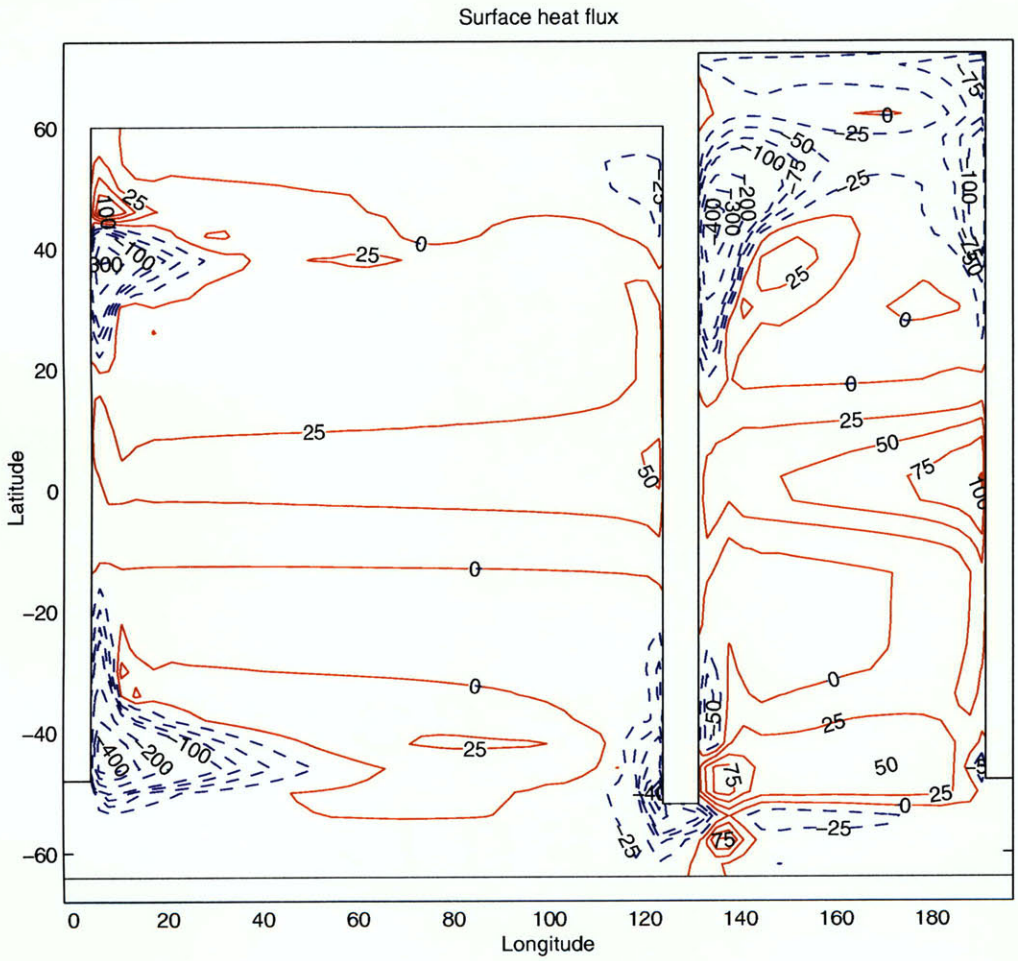

Figure -10: Control run. Surface heat flux in Wm^{-2} for diapycnal diffusivity 0.5 cm^2/s. Contour interval is 25 Wm^{-2} between -100 Wm^{-2} and 100 Wm^{-2} and 100 Wm^{-2} outside this range.

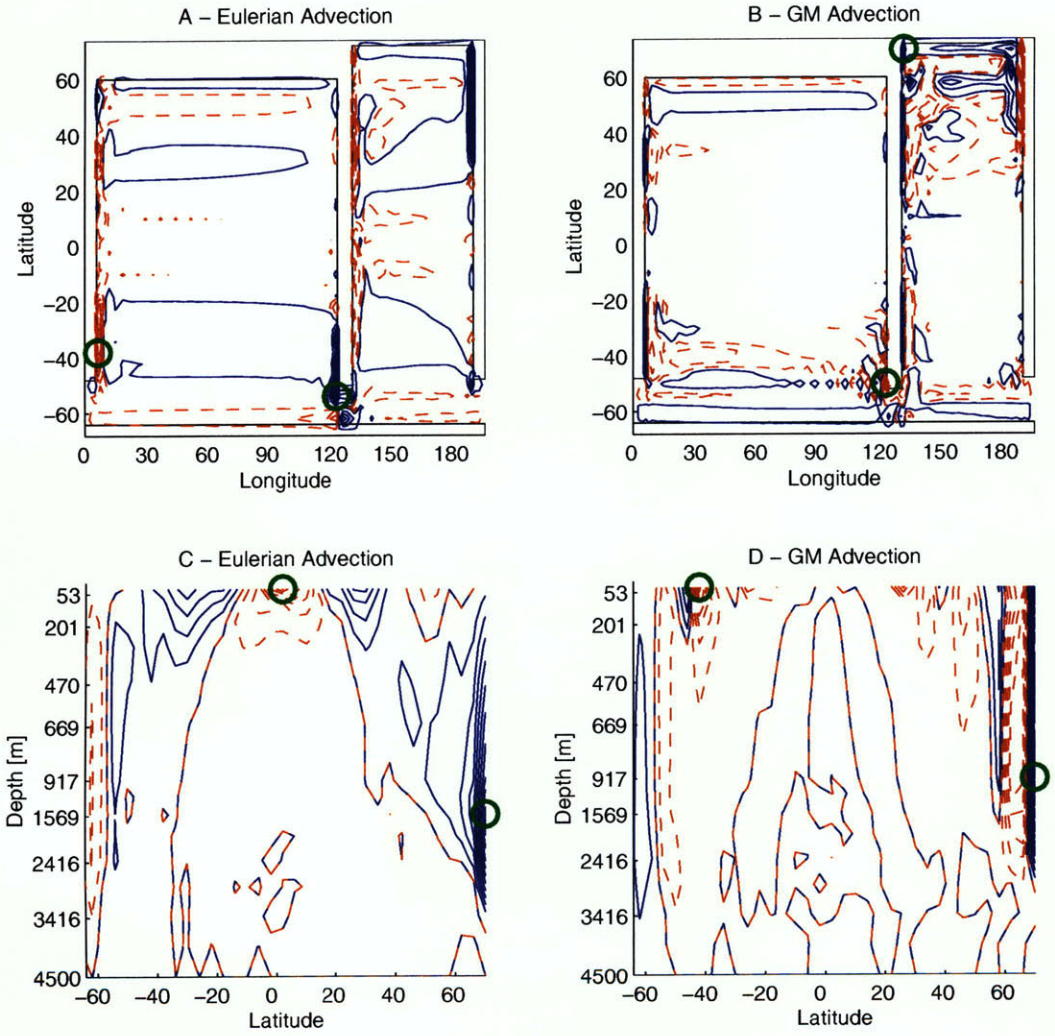

Figure -11: Control run. Eulerian (panels A, C) and GM (panels B, D) advective fluxes for diapycnal diffusivity 0.5 cm^2/s. Vertical fluxes at 250m (panels A, B) and zonal average fluxes for the global ocean (panels C, D). Solid (dashed) line for downward (upward) fluxes. The circles denote the position of the maximum and minimum.

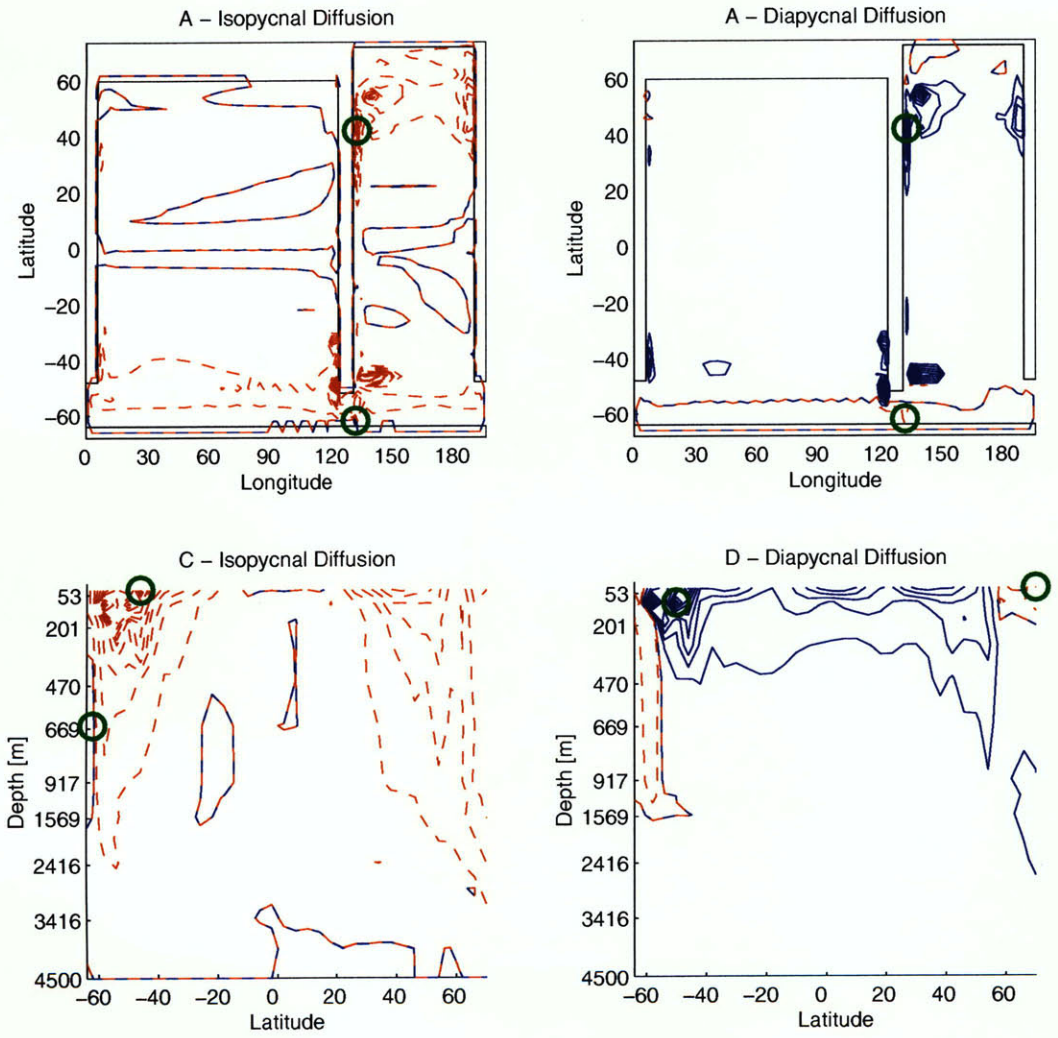

Figure -12: Control run. Isopycnal (panels A, C) and diapycnal (panels B, D) diffusive fluxes for diapycnal diffusivity 0.5 cm^2/s. Vertical fluxes at 250m (panels A, B) and zonal average fluxes for the global ocean (panels C, D). Solid (dashed) line for downward (upward) fluxes. The circles denote the position of the maximum and minimum.

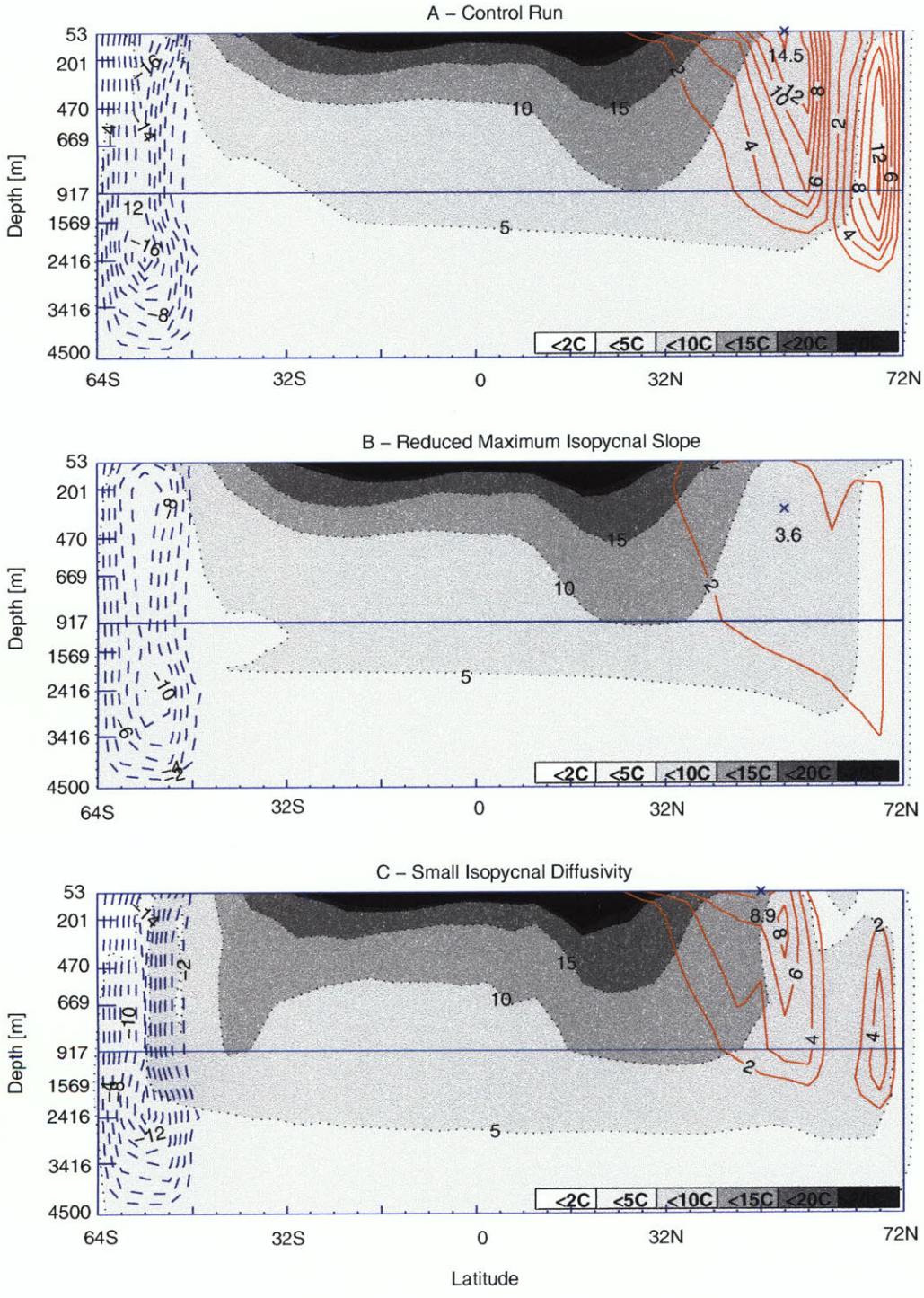

Figure -13: Bolus velocity streamfunction in the Atlantic Ocean for diapycnal diffusivity 0.5 cm^2/s. Control run (A), Reduced Maximum isopycnal Slope (B) and Small Isopycnal Diffusivity (C) experiments. In the Antarctic Circumpolar region the global streamfunction is plotted. Zonal average temperature is shaded according to the scale in panel A.

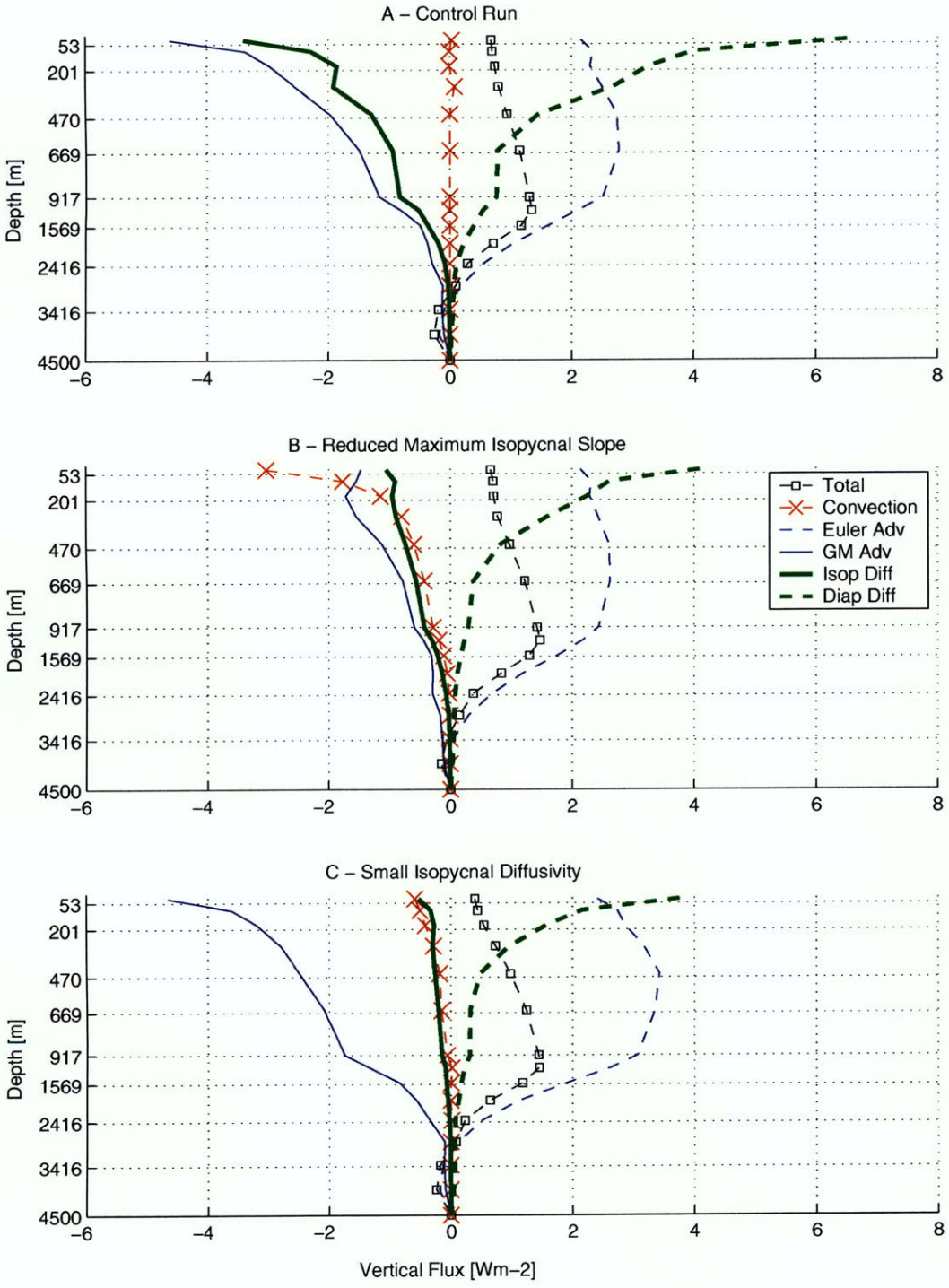

Figure -14: Vertical heat balance in the Atlantic Ocean for diapycnal diffusivity 0.5 cm^2/s. Control run (A), Reduced Maximum isopycnal Slope (B) and Small Isopycnal Diffusivity (C) experiments.

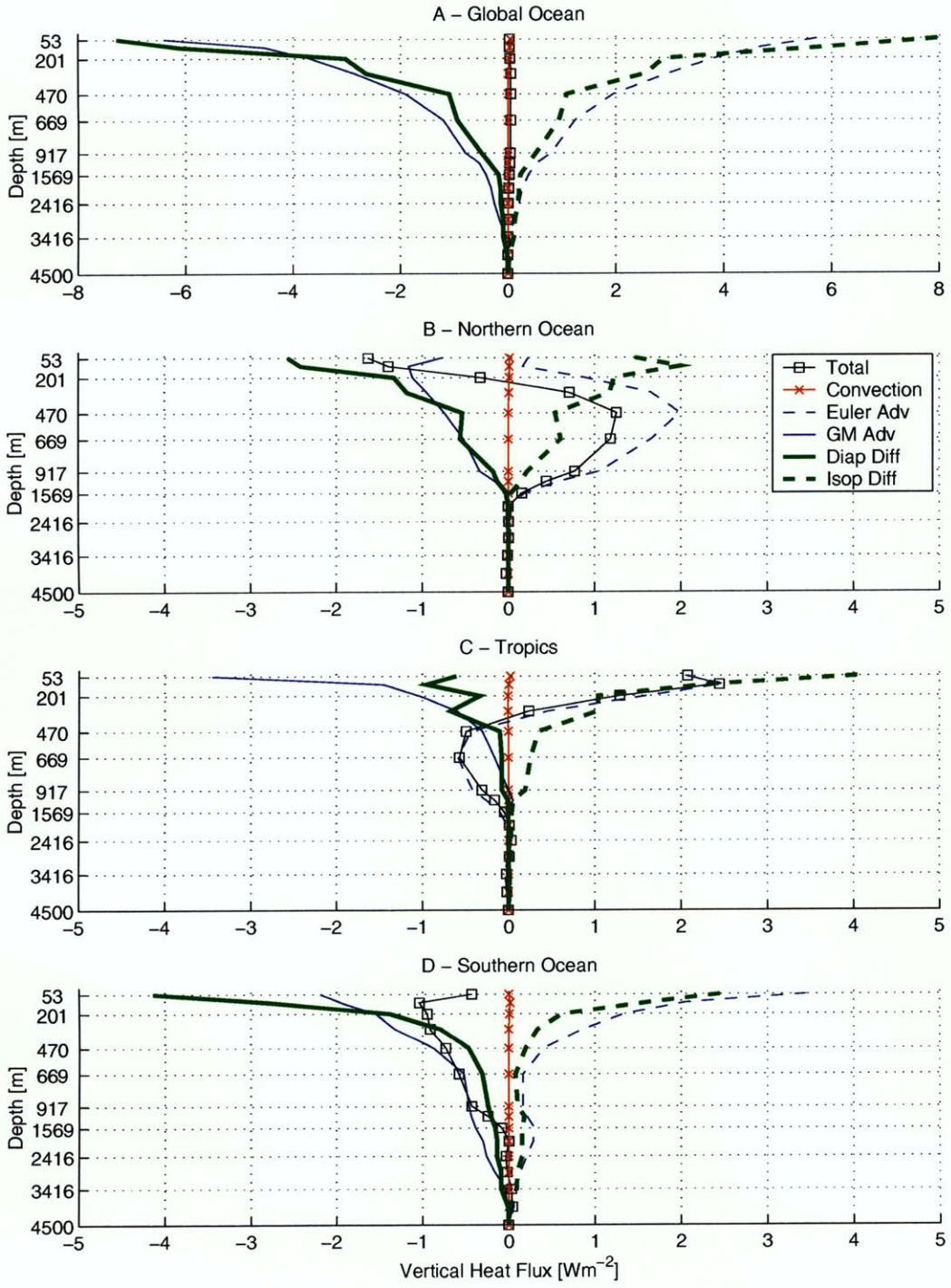

Figure -15: Control run. Vertical heat flux components for global ocean (A), Northern Ocean (B), Tropics (C) and Southern Ocean (D) for diapycnal diffusivity 0.1 cm^2/s. Positive (negative) sign for downward (upward) fluxes. Note the change of scale in panel A.

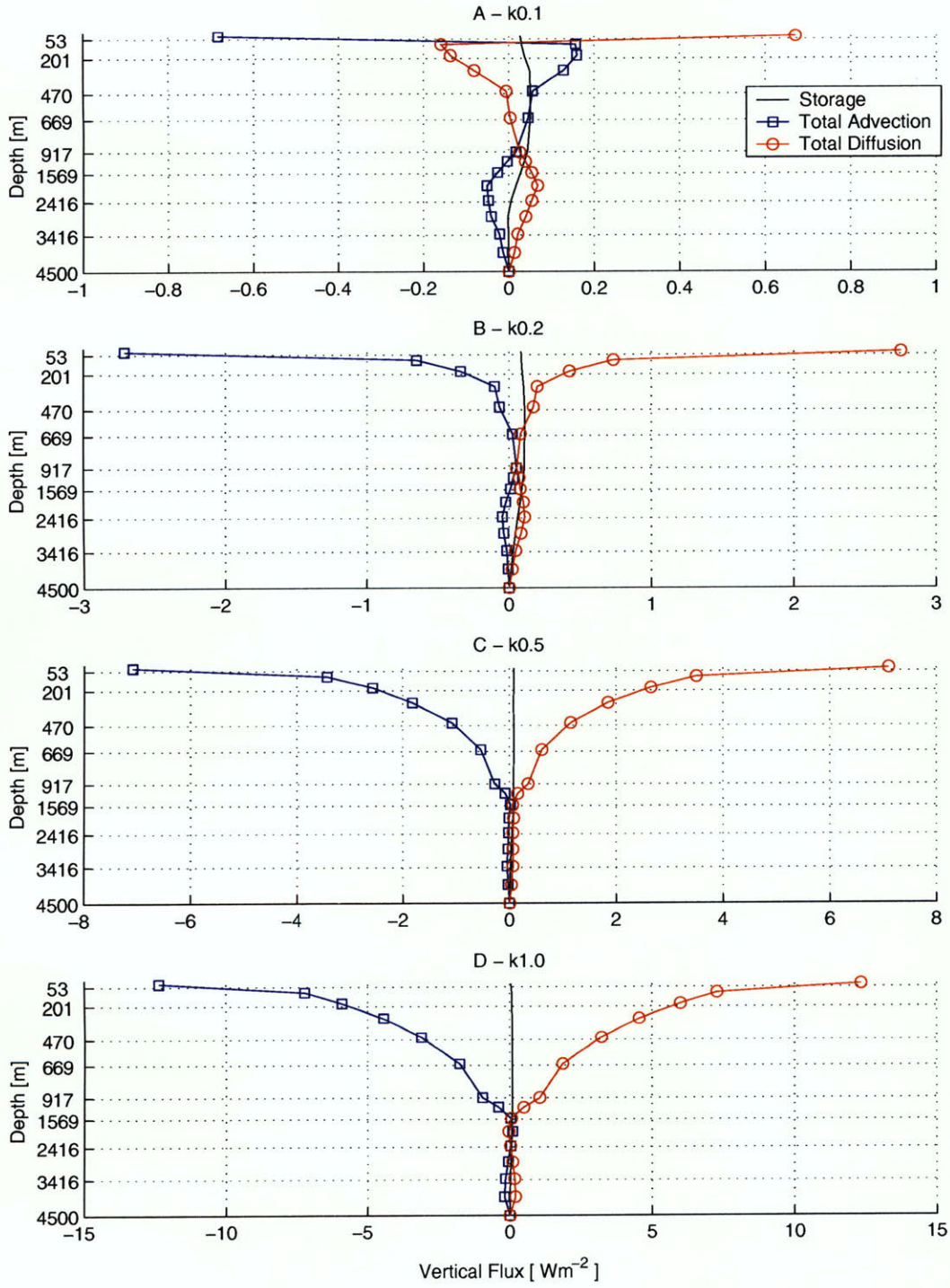

Figure -16: Heat balance for the global ocean for diapycnal diffusivity 0.1 cm^2/s (A), 0.2 cm^2/s (B), 0.5 cm^2/s (C), 1.0 cm^2/s (D). Positive (negative) sign for downward (upward) fluxes. Note the change in horizontal scales.

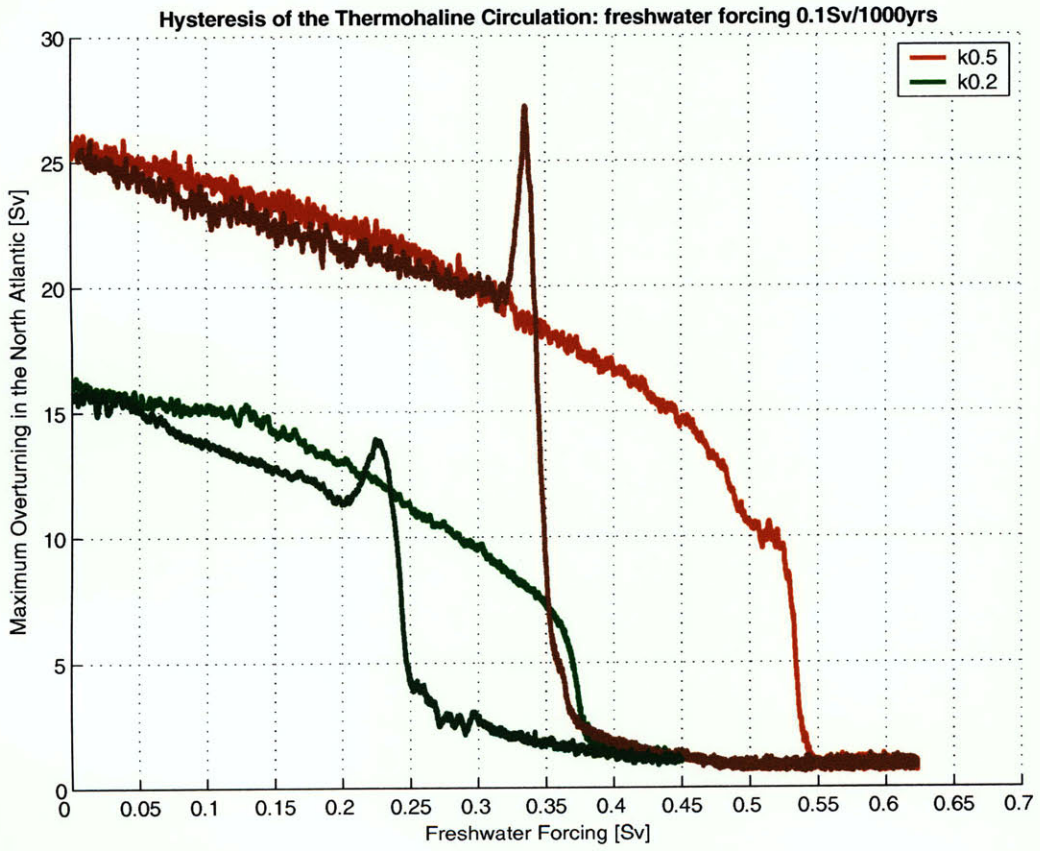

Figure -17: Hysteresis cycle of the THC for diapycnal diffusivity 0.5 cm^2/s and 0.2 cm^2/s. Data for diapycnal diffusivity 0.5 cm^2/s provided by Igor Kamenkovich.

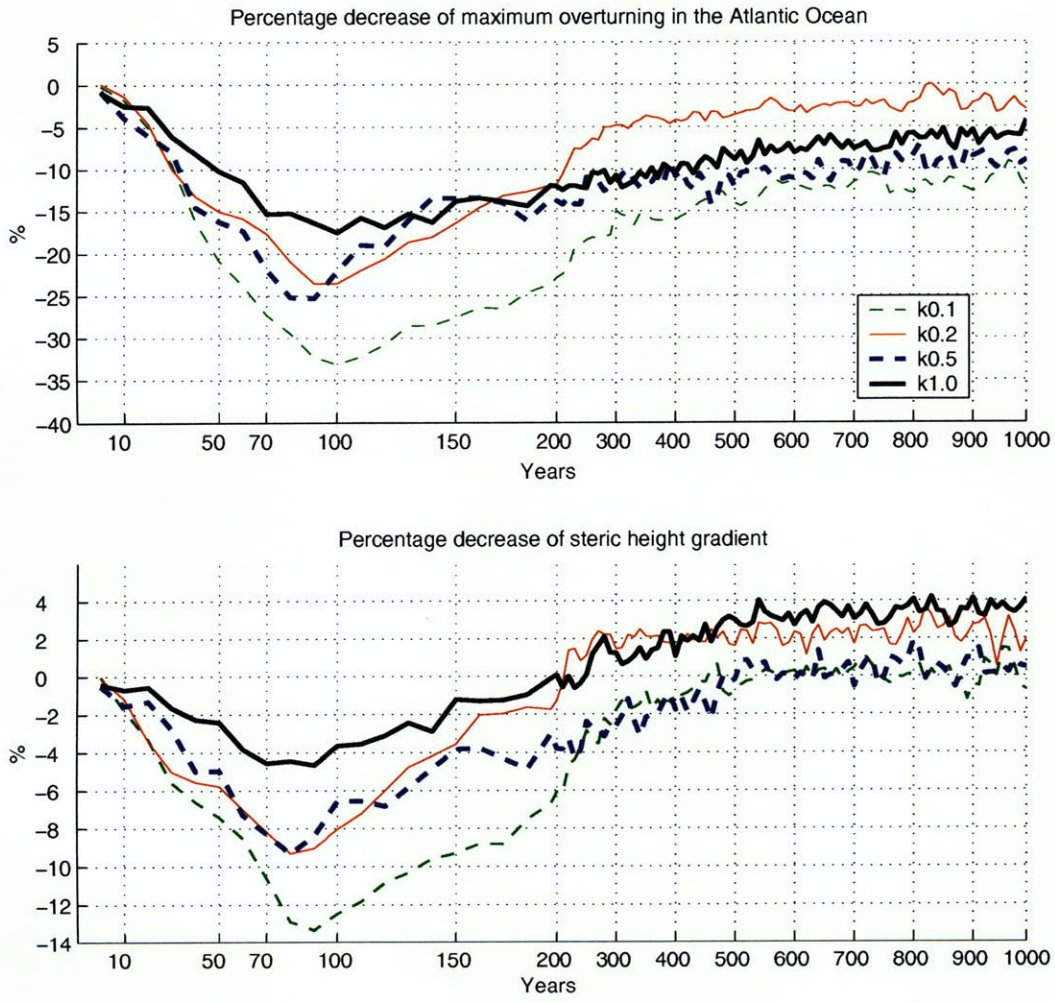

Figure -19: Percentage reduction of maximum meridional streamfunction (top) and steric height gradient (bottom) in the Atlantic Ocean for different values of the diapycnal diffusivity: diffusivity 0.1 cm^2/s thin dashed line, 0.2 cm^2/s thin solid line, 0.5 cm^2/s thick dashed line and 1.0 cm^2/s thick solid line. Note the stretching of the horizontal axis.

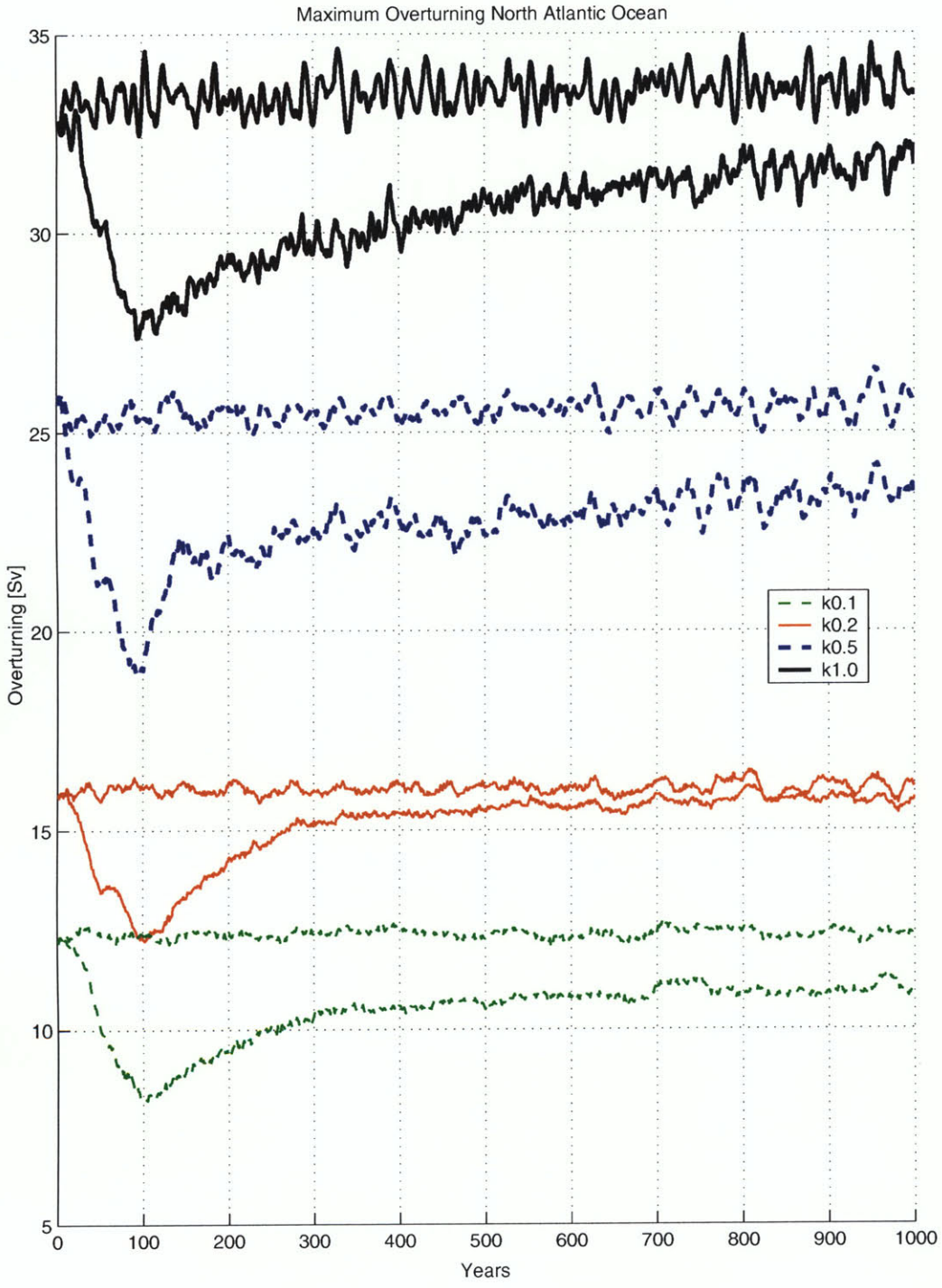

Figure -18: Maximum meridional streamfunction in the North Atlantic Ocean for different values of the diapycnal diffusivity: diffusivity 0.1 cm^2/s thin dashed line, 0.2 cm^2/s thin solid line, 0.5 cm^2/s thick dashed line and 1.0 cm^2/s thick solid line. Control run and global warming experiments are displayed.

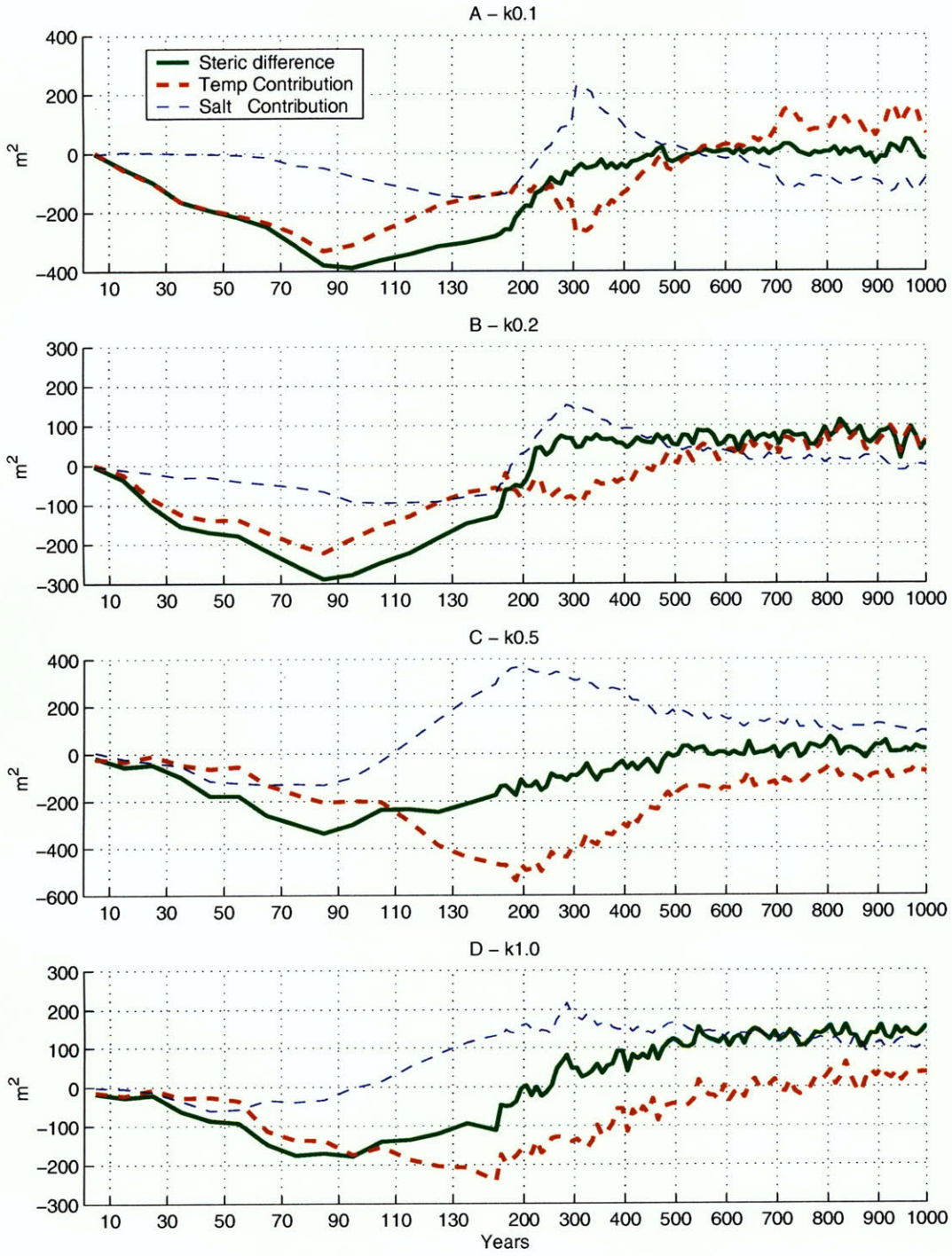

Figure -20: Steric height gradient anomaly (solid) and its temperature (thick dashed) and salinity (thin dashed) contribution in the Atlantic Ocean for different values of the diapycnal diffusivity: 0.1 cm^2/s, panel A; 0.2 cm^2/s, panel B; 0.5, cm^2/s panel C; 1.0 cm^2/s, panel D. Note the stretching of the horizontal axis.

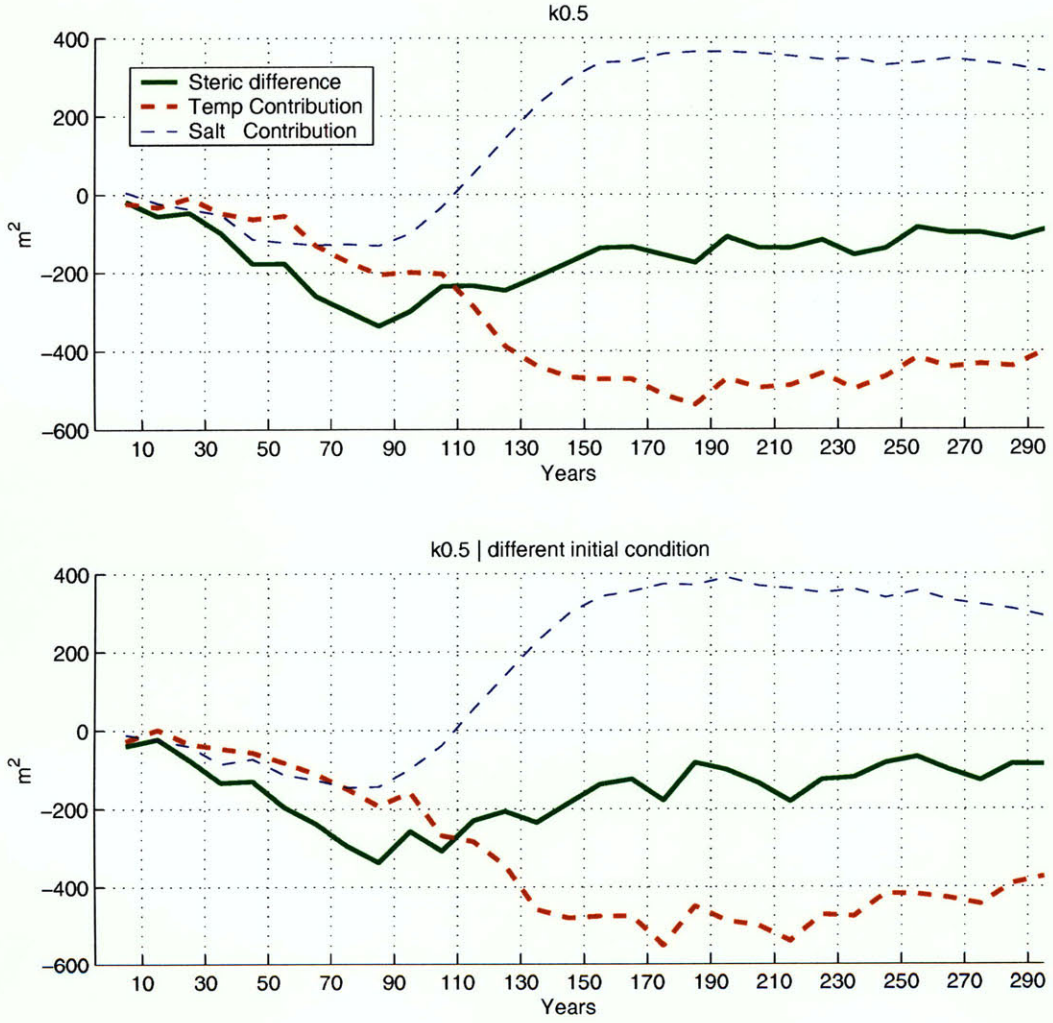

Figure -21: Steric height anomaly (solid) and its temperature (thick dashed) and salinity (thin dashed) contribution in the Atlantic Ocean for diapycnal diffusivity 0.5 cm^2/s. The two realizations differ in the initial condition taken at year 0 (top) and year 10 (bottom) of the control run.

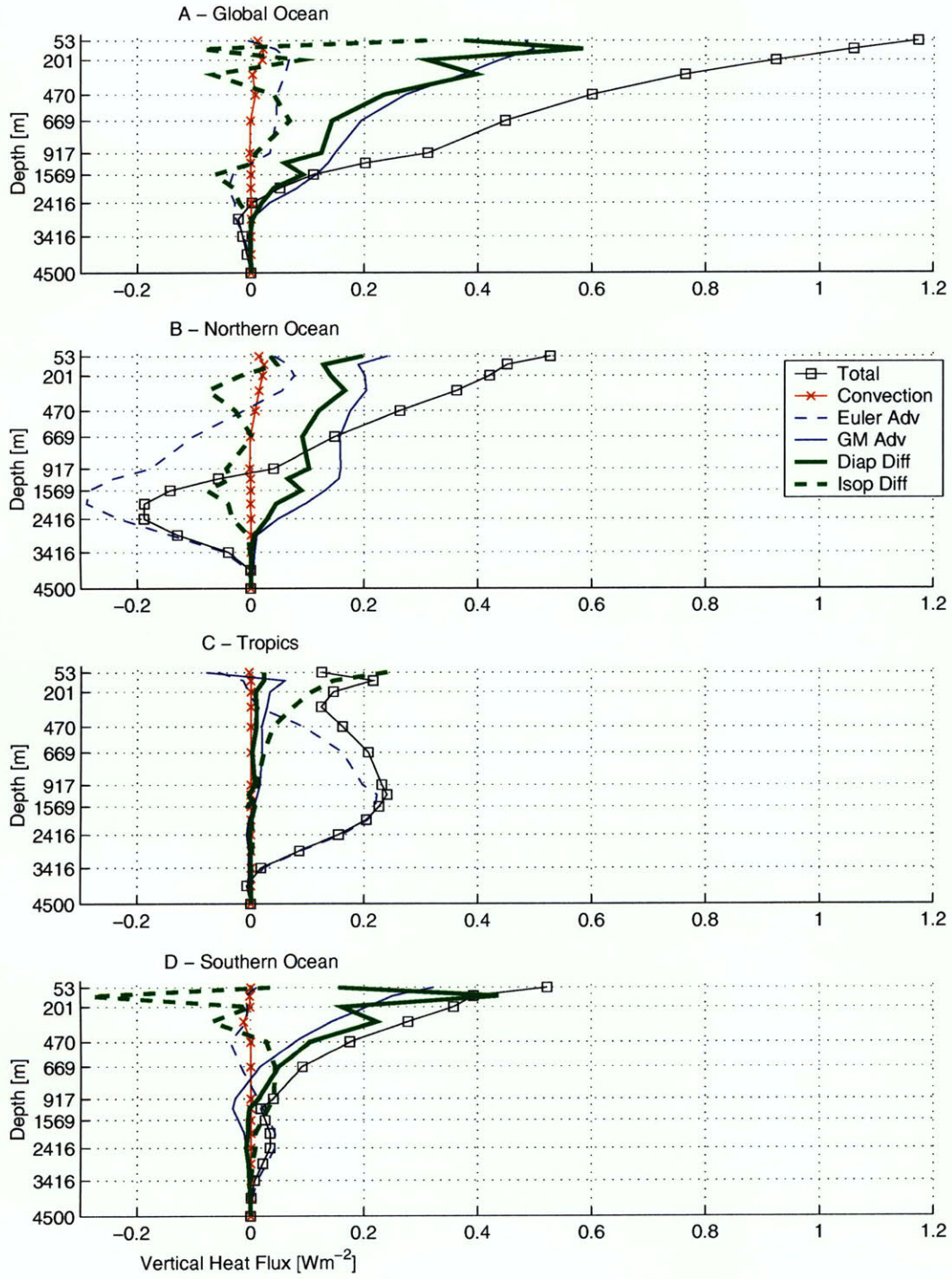

Figure -22: Global warming experiment. Vertical heat flux anomalies for global ocean (A), Northern Ocean (B), Tropics (C) and Southern Ocean (D) for diapycnal diffusivity 0.5 cm^2/s. Positive (negative) sign indicates increase (decrease) in downward flux or decrease (increase) in upward flux depending on the direction of the flux at equilibrium (see fig. -8). Average from years 1 to 75.

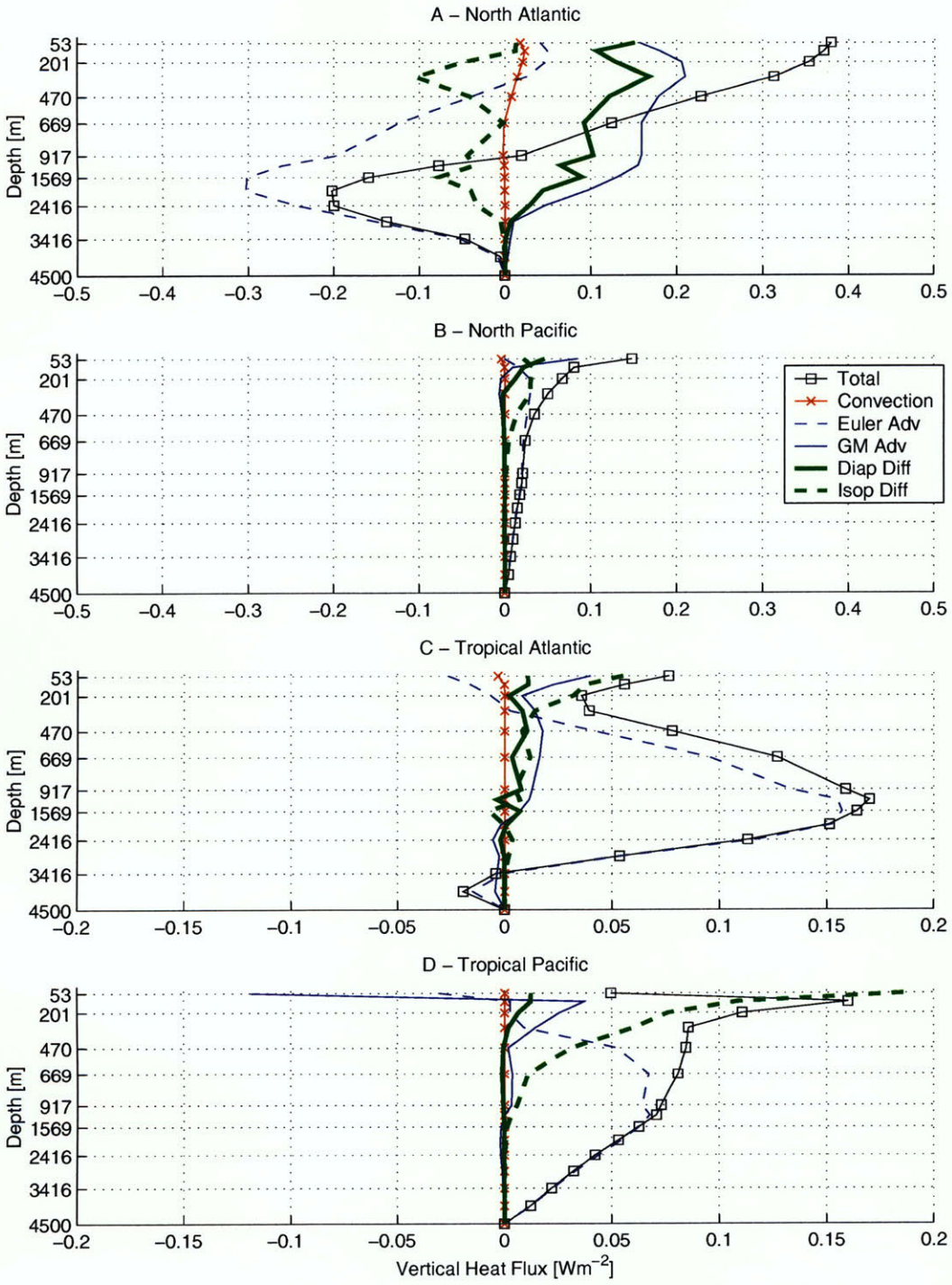

Figure -23: Global warming experiment. Vertical heat flux anomalies for the North Atlantic (A), North Pacific (B), tropical Atlantic (C) and tropical Pacific (D) for diapycnal diffusivity 0.5 cm^2/s. Positive (negative) sign indicates increase (decrease) in downward flux or decrease (increase) in upward flux depending on the direction of the flux at equilibrium (see fig. -9). Note the change of scale in the horizontal axis. Average from years 1 to 75.

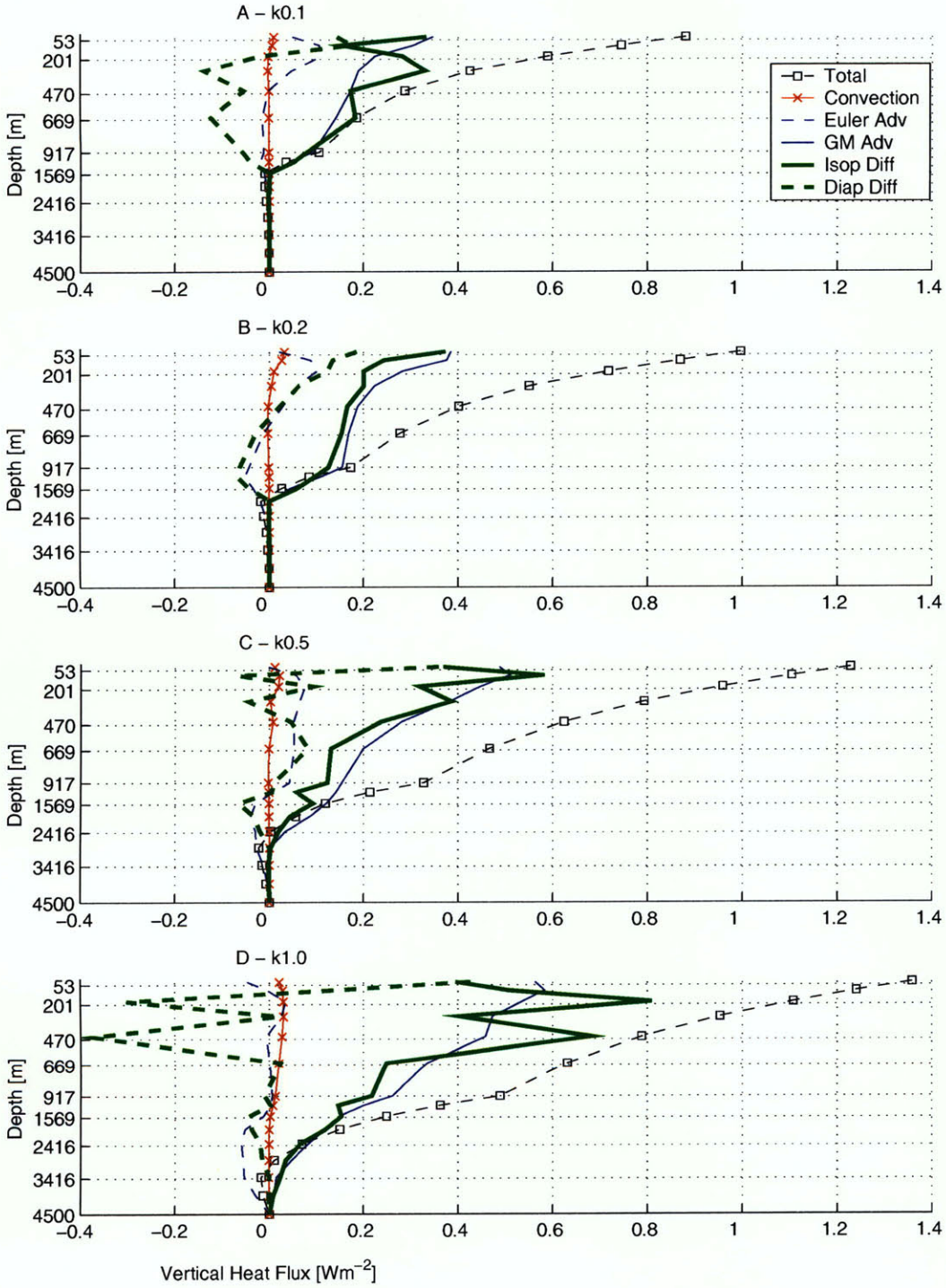

Figure -24: Heat balance anomaly due to global warming for the global ocean and for diapycnal diffusivity 0.1 cm^2/s (A), 0.2 cm^2/s (B), 0.5 cm^2/s (C), 1.0 cm^2/s (D). Positive (negative) sign indicates increase (decrease) in downward flux or decrease (increase) in upward flux depending on the direction of the flux at equilibrium (see fig. -16). Average from years 1 to 75.

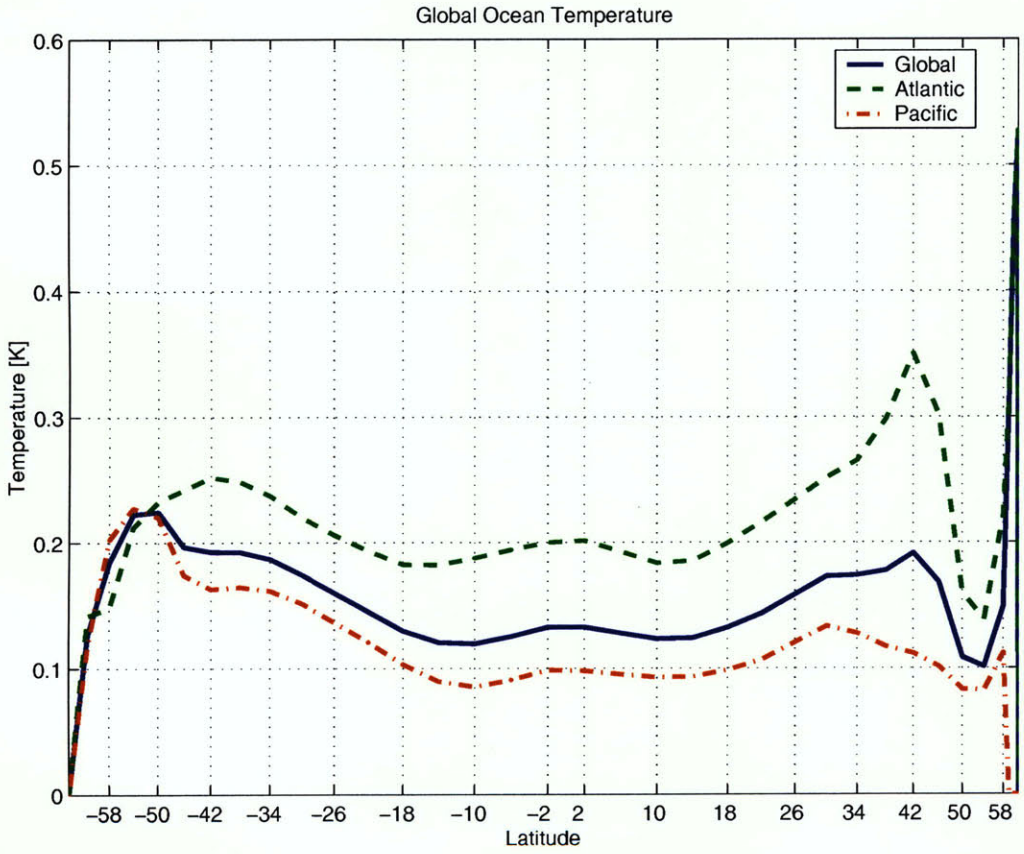

Figure -25: Meridional distribution of global ocean temperature anomaly at the time of CO_2 doubling for diapycnal diffusivity 0.5 cm^2/s.

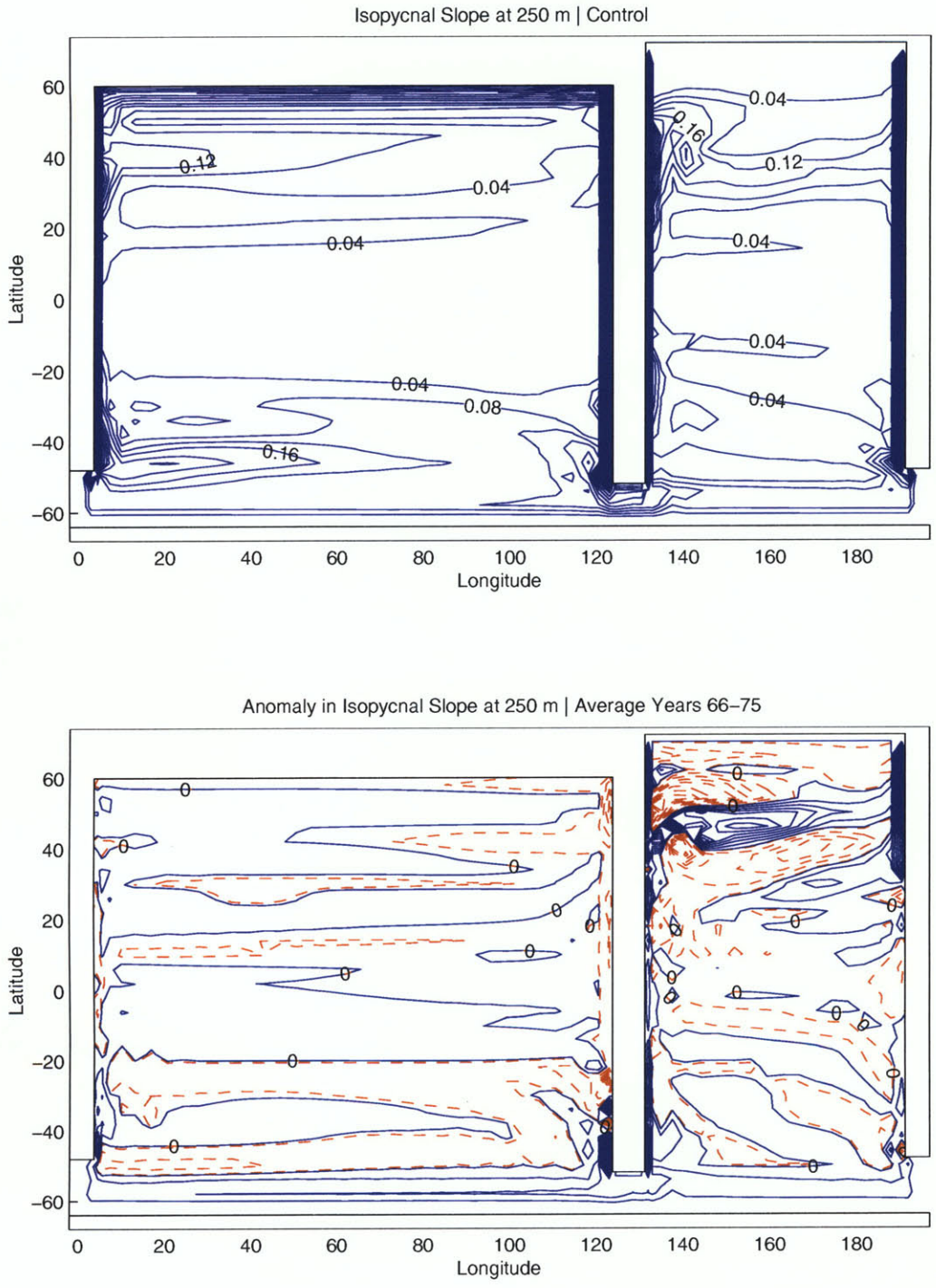

Figure -26: Modulus of the isopycnal slope (top) and its anomaly due to global warming (bottom) at 250m depth for diapycnal diffusivity 0.5 cm^2/s. Solid line denotes positive values and dashed line denotes negative values.

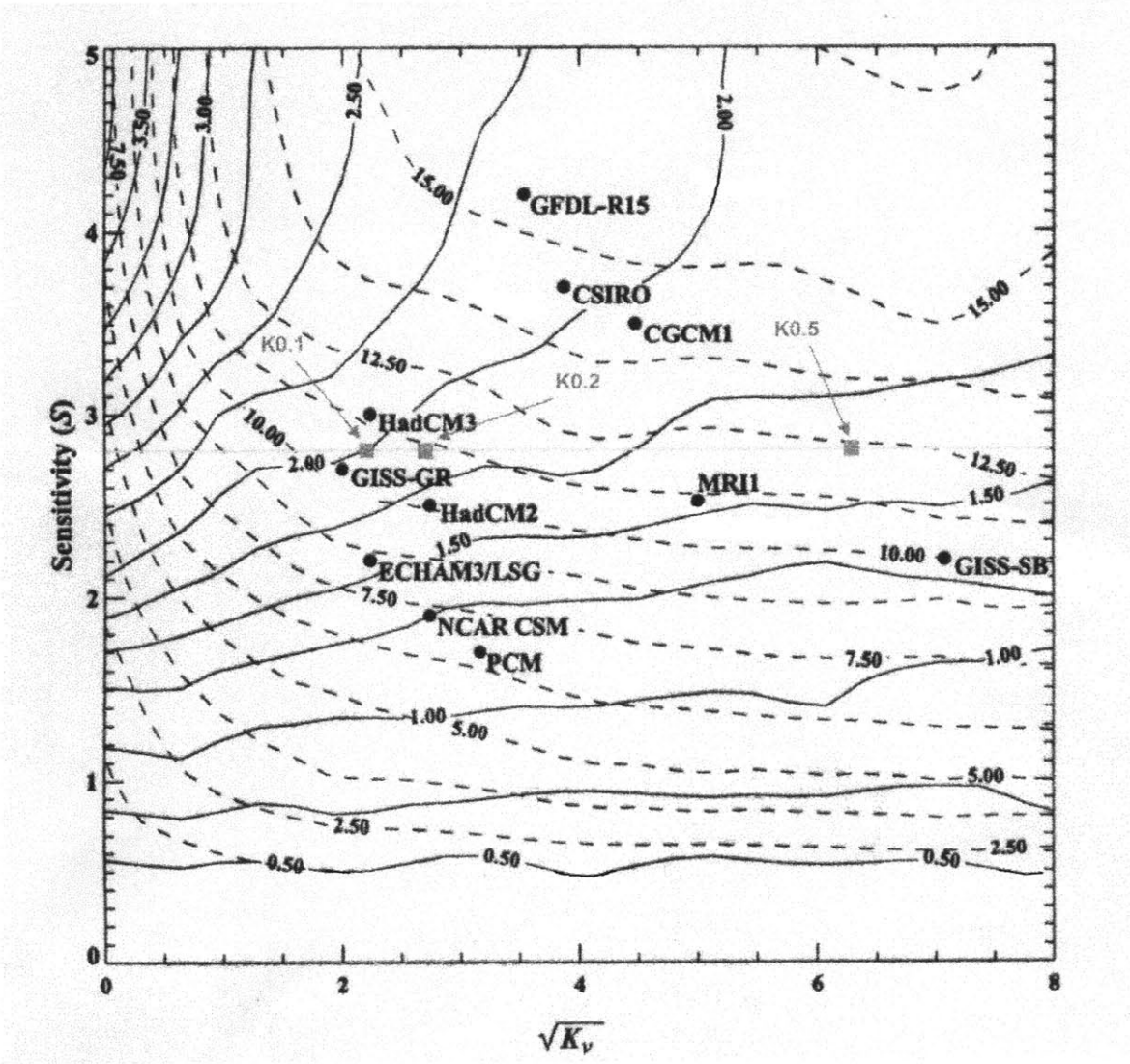

Figure -27: Dependence of SAT and SLR at the time of doubling of CO_2 as a function of climate sensitivity (S) and effective diffusivity (K_v). Black circles represents the position of CMIP2 models in the parametric space while the gray squares represents the position of the MIT-EMIC for different values of the diapycnal diffusivity. Figure adapted with permission from Sokolov et al. (2003).

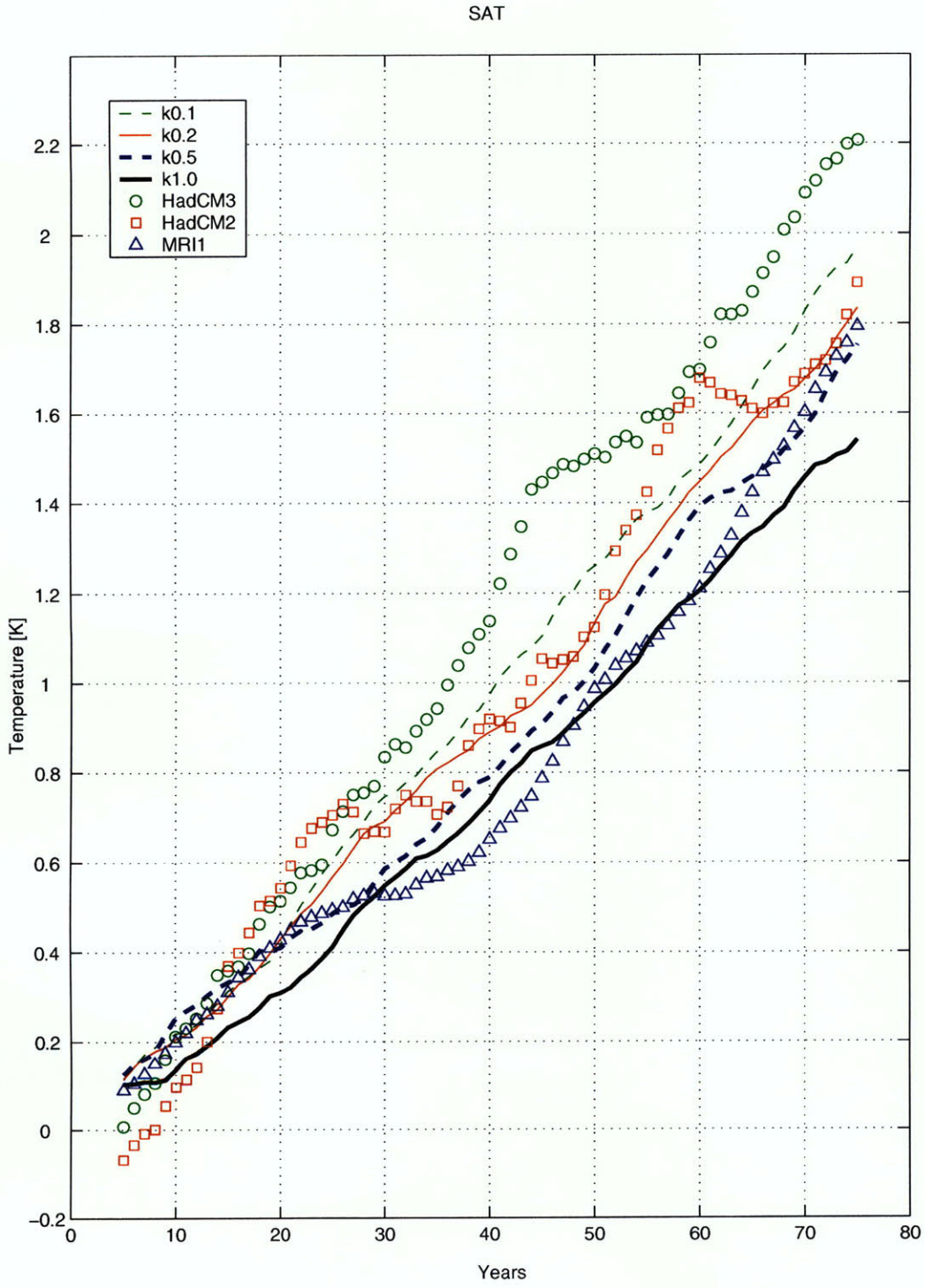

Figure -28: Global average Surface Air Temperature for MIT-EMIC with different diapycnal diffusivity and CMIP2 models MRI1 (triangle), HadCM2 (square) and HadCM3 (circle). 10 years running mean.

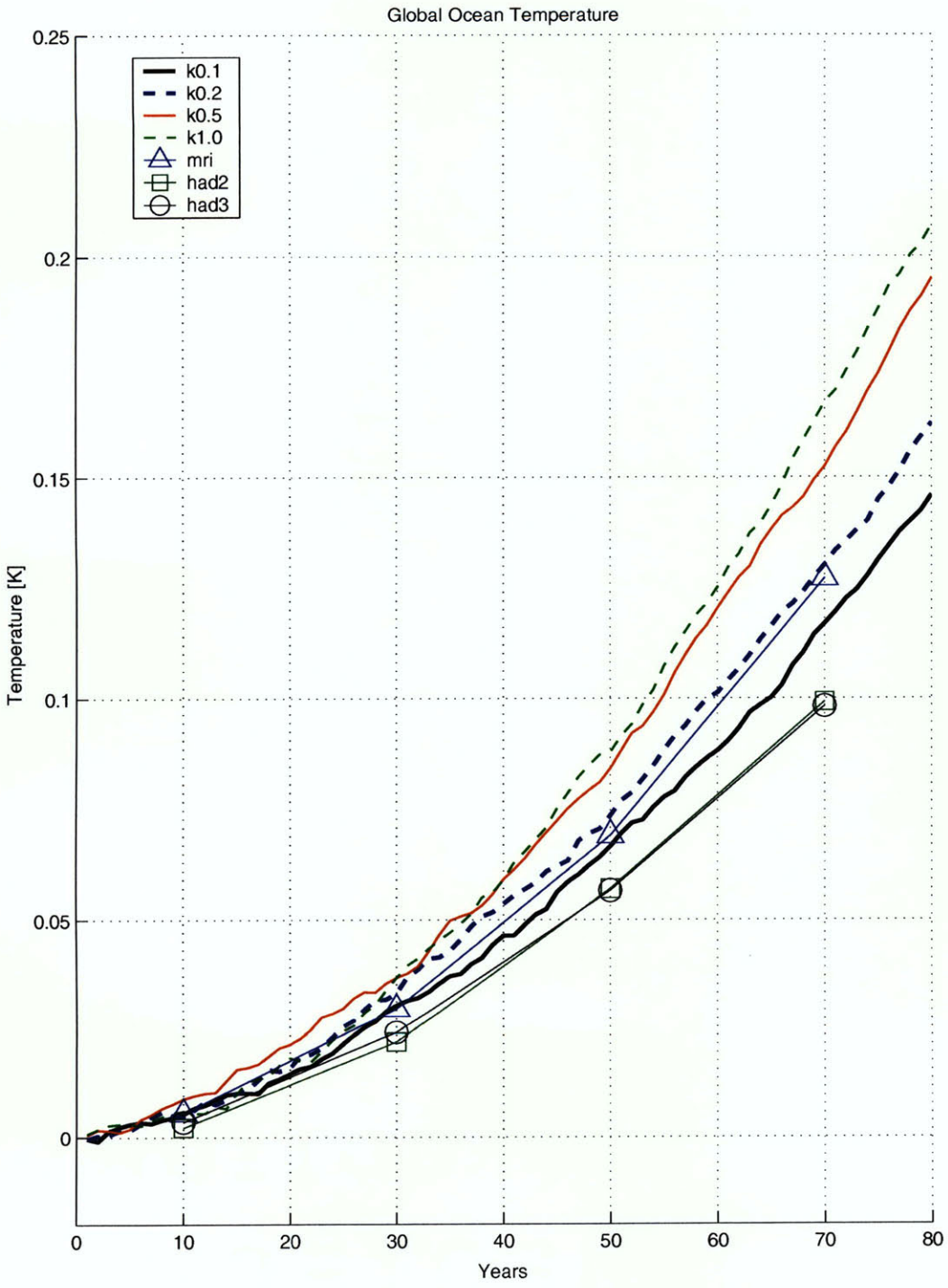

Figure -29: Global average ocean temperature for MIT-EMIC with different diapycnal diffusivity and CMIP2 models MRI1 (triangle), HadCM2 (square) and HadCM3 (circle).